NASA TM X-128

TECHNICAL MEMORANDUM

X-128

TRANSONIC AND SUPERSONIC EJECTION RELEASE CHARACTERISTICS OF SIX DYNAMICALLY SCALED EXTERNAL-STORE SHAPES FROM AN 0.086-SCALE MODEL OF A CURRENT FIGHTER AIRPLANE

By William F. Hinson

Langley Research Center
Langley Field, Va.

NATIONAL AERONAUTICS AND SPACE ADMINISTRATION

WASHINGTON December 1959

1C

NATIONAL AERONAUTICS AND SPACE ADMINISTRATION

TECHNICAL MEMORANDUM X-128

TRANSONIC AND SUPERSONIC EJECTION RELEASE CHARACTERISTICS OF SIX DYNAMICALLY SCALED EXTERNAL-STORE SHAPES FROM AN 0.086-SCALE MODEL OF A CURRENT FIGHTER AIRPLANE*

By William F. Hinson

SUMMARY

An investigation has been made to determine the capability of a current fighter airplane to satisfactorily eject external stores at transonic and supersonic speeds. These stores include a bomb of fineness ratio 8.33 (bomb 1), a bomb of fineness ratio 7.57 (bomb 2), a weapons pod of fineness ratio 9.20, a pylon-mounted fuel tank, a pylon, and a wing-tip mounted fuel tank.

Satisfactory releases were obtained with bomb 1 (free-stream Mach number of 1.98 and high altitudes) and with bomb 2 (free-stream Mach number of 0.9 and low altitudes). Unsatisfactory releases were obtained with the basic body configuration of the weapons pod at a free-stream Mach number of 1.39 and high altitude. However, a satisfactory release, at the same conditions above, was obtained by the addition of a horizontal-tail fin. At a free-stream Mach number of 1.39, clean separation was obtained with an empty wing-tip tank (high altitude) and with an empty pylon tank (high altitude). At low altitude the pylon tank experienced large negative pitch angles in the immediate vicinity of the airplane model. This caused the tail of the pylon tank to remain close to the wing trailing edge for approximately 25 milliseconds (model scale) after release. Clean pylon separation was obtained at high subsonic speeds (low altitudes) and supersonic speeds (high altitudes). After release the pylon experienced erratic motions, but at no time came close to striking the airplane model.

Author

---

* Title, Unclassified.

[redacted]

INTRODUCTION

Among the many problems associated with the operation of aircraft has been the one of store separation. This problem has become acute with the increase of aircraft speeds from high subsonic velocities to supersonic velocities. Low density stores, such as empty external fuel tanks, which have a low relative density ratio and low moment of inertia, react readily to the influence of aerodynamic forces and moments. This reaction often causes the store to come in contact with the carrying aircraft after release.

To extend the range and mission capability of a current fighter airplane, several external stores were developed. These stores include fuselage-weapons stores, pylon-mounted fuel tanks, and wing-tip mounted fuel tanks.

The purpose of the present investigation was to determine the capability of the current fighter airplane to satisfactorily eject these externally carried stores at transonic and supersonic speeds. Therefore, a study of the store oscillations and trajectories which occurred near the airplane model after release was made. The stores were ejected at free-stream Mach numbers of 0.9, 1.39, and 1.98. Approximate altitudes simulated were sea level, 7,800, 11,000, 25,000, and 40,000 feet.

This investigation was made in the 27- by 27-inch preflight jet of the NASA Wallops Station using 0.0858 dynamically scaled models. Reynolds number per foot for the models tested was approximately 7×10^6 to 14×10^6.

SYMBOLS

a	acceleration, g units or ft/sec^2
d_s	maximum store diameter, in.
E	ejection energy, produced by detonation of an electric squib, model, and prctotype
F	force, lb
h_a	simulated altitude
I_y	store moment of inertia about pitch axis, $slug\text{-}ft^2$
L	characteristic length

[redacted]

l_s store length, in.

M_∞ free-stream Mach number

m model mass, slugs

p static pressure, lb/ft^2

q dynamic pressure, lb/ft^2

S ejector piston stroke, in.

Δt time interval between frames on microflash photographs, milliseconds

w weight, lb

x_{cg} center of gravity, measured from nose of store, in.

x_s horizontal coordinate of store displacement, with origin at the store center of gravity at initial release, positive downstream, in.

y_s coordinate of lateral store displacement (wing-tip tank only) with origin at center of gravity at initial release, positive to the starboard, in.

z_s vertical coordinate of store displacements, with origin at the store center of gravity at initial release, positive down, in.

α_w wing angle of attack, deg

θ_s store pitch angle with respect to the horizontal, deg

λ scale factor, $\frac{L_M}{L_P}$

ψ_s store yaw angle with respect to vertical plane, deg

Subscripts:

M model

P prototype

∞ free-stream conditions

[redacted]

MODELS AND APPARATUS

Stores

Figures 1 to 6 show model sketches of the dynamically scaled stores tested, which consist of three fuselage-weapons stores, a pylon mounted fuel tank, a pylon, and a wing-tip tank.

Bomb 1.- Bomb 1 (fig. 1(a)) is a symmetrical streamlined bomb with a fineness ratio of 8.33 and cruciform tail fins. Due to the small clearance between the tail fins of this store and the ventral fin of the airplane, it was necessary to install the store with its fins rotated 6° counter clockwise.

L
5
4
5

Bomb 2.- Bomb 2 (fig. 1(b)) is a streamlined bomb with a fineness ratio of 7.57. The tail fins with the plan form as shown in figure 5 were rotated 30° downward from the horizontal plane and given a small negative angle of incidence. The full-scale bomb carries a parachute in its tail section. The parachute is deployed after release to help stabilize the bomb and allow a slower descent. The deployment of the parachute was not simulated in this investigation.

Weapons pod.- The weapons pod (fig. 1(c)) has a relatively large hemispherical nose followed by a conical section. The midsection is cylindrical with a conical boattailed afterbody. This configuration was tested with and without tail fins. The fineness ratio was 9.20.

Pylon.- The plan form of the pylon is shown in figure 2. Basically it is used for the purpose of mounting a fuel tank. This pylon had a sweptback leading edge of 62.5° with a straight nonswept trailing edge. The pylon thickness-to-chord ratio at the wing lower surface is 5.1 percent and at the pylon tank upper surface, 3.3 percent.

Pylon fuel tank.- A pylon tank is carried under each wing, and each has a capacity of 200 gallons (full scale). The tank is attached to the above described pylon. The distance between the lower surface of the wing and the upper curvature of the tank was 1.17 inches (model scale). The tank is carried in a nose-down attitude of approximately 3° relative to the wing chord line. A model sketch and tail fin arrangement of the pylon tank is shown in figure 3. The fineness ratio was 10.25.

Wing-tip tank.- The wing-tip tank is fitted over the wing tip by means of a recessed slot in the tank body. The capacity of the wing-tip tank is 165 gallons (full scale). A vortex generator is mounted on the forward portion of the tank body for the purpose of improving the flow characteristics over the wing tip when the tip tank is installed. A model sketch including the vortex generator and tail fin configuration is shown in figure 4. The tank fineness ratio was 10.25.

Fin plan forms.- The fin plan forms with dimensions are shown in figures 5 and 6.

Store installation, ejection, and construction.- Store installation and ejection were accomplished through the use of a piston-cylinder combination as shown in figure 7. In some cases the piston was attached to the store model and the cylinder to the airplane model. In other cases the reverse was true. In either case, after the piston was fitted in the ejection cylinder, a pin was inserted in a hole drilled through the ejection cylinder and piston. Guide pins in the store body were used for proper alinement. Electric squibs were used to force the piston which in turn sheared the inserted pin and ejected the store. The ejection energy was scaled by the expression

$$E_M = E_P \frac{p_M}{p_P} \lambda^3$$

This expression is derived in the appendix.

The store models were constructed of solid duralumin and ballasted with tungsten except for two models which were constructed from reinforced plastic. An attempt was made to construct all the store models from reinforced plastic, but most of these models failed under the aerodynamic loads encountered in the supersonic airstream. The data from two reinforced plastic models (pylon tanks) which did not fail have been presented herein.

Airplane Model

Figure 8(a) shows a 0.0858-scale model of the current fighter airplane. The airplane model was attached to a single strut (fig. 8(a)) which was free to be moved only in the vertical direction between track rollers in the beam support.

In some tests it was necessary to impart an upward acceleration to the airplane model at the instant of store release. When this was the case the upward acceleration of the airplane model was obtained from lift and a hydraulic cylinder which was attached to the upper end of the vertical fuselage strut. Deceleration of the airplane model near the end of its upward movement was obtained by two damping hydraulic cylinders mounted on the beam support (fig. 9).

The nose of the airplane fuselage was placed approximately 2 inches downstream from the nozzle exit.

Preflight Jet

All tests were made in the 27- by 27-inch preflight jet of the NASA Wallops Station (ref. 1) in which the stagnation pressures and

temperatures could be varied. The Mach number of the test was changed by the use of interchangeable nozzle blocks. The complete test setup is shown in figure 9.

Photography

High-speed microflash photographs were made of the store ejections. Lighting was supplied by a series of flashbulbs which were electronically timed to overlap. The film was exposed through narrow radial slits in a rotating disk placed in front of the camera lens. The time interval between exposures varied between tests and is listed in table I.

TESTS

Dynamic Similarity

Two basic methods of obtaining dynamic similarity were employed in the present tests. These methods are (1) light model method, and (2) heavy model method. Both methods (ref. 1) require that the nondimensional radii of gyration, Mach number, air properties, air temperature for model and full-scale configuration be equal and that model and full-scale configuration be geometrically similar.

Light model method.- Using the light model method the model weight and moment of inertia are defined by the following expressions:

$$w_M = \left(\frac{L_M}{L_P}\right)^3 \frac{p_M}{p_P} w_P \qquad (1)$$

and

$$I_{y,M} = \left(\frac{L_M}{L_P}\right)^5 \frac{p_M}{p_P} I_{y,P} \qquad (2)$$

With this method of scaling, the time to travel a distance of one characteristic length in the streamwise or x-direction, and the period and time to damp the short-period longitudinal oscillation are proportional to the characteristic length. The aerodynamically produced accelerations are inversely proportional to the characteristic length. Inasmuch as the gravity-induced acceleration cannot respond to scale changes in a manner similar to the aerodynamically-induced accelerations, the vertical acceleration, velocities, and displacements are deficient. One way of minimizing this deficiency is to accelerate the parent model vertically

at a rate equal to $\left(\frac{L_P}{L_M} - 1\right)g$, at the instant of store release. The trajectory of the model with respect to the parent model then closely approximates that of the full-scale configuration. This method (modified light model method identified herein as M-LM) was used in most of the present tests.

Heavy model method.- In the heavy model method (H-M) the model weight and moment of inertia are given by the following expressions:

$$w_M = \left(\frac{L_M}{L_P}\right)^2 \frac{p_M}{p_P} w_P \tag{3}$$

$$I_{y,M} = \left(\frac{L_M}{L_P}\right)^4 \frac{p_M}{p_P} I_{y,P} \tag{4}$$

In this method, the aerodynamically produced accelerations are independent of the scale, whereas the period and velocity are proportional to the square root of the scale. In the present test, due to density limitations of available materials, some of the stores on which the heavy model method was used were lighter than the required weight. Therefore, to circumvent this deficiency in weight, the parent model was given an upward acceleration. The value of acceleration was given by the following expression:

$$\text{acceleration in g's} = \frac{w_{required}}{w_{actual}} - 1 \tag{5}$$

Therefore, the store weights were simulated but the moments of inertia were in error.

Test Method and Accuracies

In all tests where the airplane model was accelerated upward the airplane model, with store attached, was held stationary in the tunnel airstream until the tunnel reached operating conditions. Then at the same time that the airplane model was accelerated upward, the store was ejected downward. In the test where the airplane model was not accelerated it was held stationary in the tunnel airstream during the complete test. (See remarks column, table I.) The release of the store was synchronized with a series of flashbulbs and the opening of a camera shutter. Thus, with a slotted spinning disk in front of the opened camera shutter, the camera took a scaled time trajectory of the free-falling store on a piece of 8- by 10-inch film. Table I lists each test along with pertinent conditions.

A summary of the estimated maximum probable errors for the tests and store models is presented in the following table:

x_s/d_s	±0.004
z_s/d_s	±0.004
θ_s, deg	±0.5
p, lb/in.	±0.01
M_∞	±0.01
E_M, percent	±0.10
$I_{y,M}$:	
Bomb 1, (percent too small)	47.7
Bomb 2, (percent too small)	44.8
Pylon, (percent too small)	5.05

RESULTS AND DISCUSSION

The results are presented in the form of microflash photographs, along with plots of the pitch oscillations and trajectories. The pitch oscillation and trajectory data were measured from the photographs. Zero time was taken to correspond to the detonation of the electric squib.

Figures 10 through 15 present the photographs with the conditions of the particular test. A bottom view photograph is shown for the purpose of indicating lateral deviation and angle of yaw.

Figures 16 through 20 show time-history plots of the store oscillations and displacements. In the tests where the airplane model was accelerated, the trajectories have been corrected for the relative distance between the airplane model and the position of the ejected store.

Ejections using bomb 1 were considered satisfactory if the bomb experienced pitch amplitudes not exceeding specified ±12° limits, with the store following a downward trajectory while immersed in the tunnel airstream.

Desired maximum positive pitch amplitudes not exceeding 45° in 0.4 second (full scale) (0.033 millisecond model scale) after release were specified for bomb 2. At this time after release the parachute described above would be fully deployed and effective.

All other store ejections were considered to be satisfactory if clean separation from the airplane model was experienced.

Bomb 1 Ejections

The photographs of the bomb 1 ejections (fig. 10) show satisfactory releases were obtained at the conditions stated. The measured data (fig. 16(a)), with $\alpha_w = 1^\circ$, indicate maximum pitch amplitudes of -9° to 6° were obtained in test 1. A repeat of test 1 (test 2) shows that the store pitch amplitudes repeat within 4°. The store trajectories appear identical for the entire time the store was immersed in the tunnel airstream.

L
5
4
5

Changing the wing angle of attack to 0.6° (fig. 16(b)) indicated no significant change in the store pitch characteristics. A small deviation is noted in the trajectory of the repeat of test 3 (test 4). This deviation is attributed to not obtaining the exact upward acceleration of the airplane model in the repeat test. Also, the change in acceleration of the airplane model resulted in a change in simulated altitude.

Bomb 2 Ejections

The photographs of the bomb 2 ejections (fig. 11) show satisfactory separation at the conditions stated. The measured data presented in figure 17 indicate a maximum pitch amplitude of 16° for approximately eight store diameters (1200 milliseconds after release, full scale) below the release point (test 5). Test 6 is a repeat of test 5 and shows the store pitch amplitudes repeat within 4° for the first eight store diameters below the release point. The trajectories (tests 5 and 6) appear identical for the first four store diameters below the release point, after which a small deviation is noted. This deviation, as stated previously, is attributed to not obtaining the exact upward acceleration of the airplane model in the repeat test. Also this deviation resulted in a change in simulated altitude.

Weapons Pod Ejections

Using the basic body configuration, the measured data (fig. 18(a), test 7) show that the store remained in a near level flight attitude for approximately five store diameters below the release point. The store then obtained lift and experienced large positive pitch amplitudes. This caused the store to pass close to the tail of the airplane model. Therefore, test 7 was not a satisfactory test and modifications to the weapons pod were attempted. By adding weight to the tail section of the store, the center-of-gravity location was moved aft. This allowed the ejection force to be applied in front of the center-of-gravity location, $\left(x_s/d_s = 0.055\right)$. Test 8 (fig. 18(a)) shows this modification did not

improve the flight characteristics of the store. Test 9 (fig. 18(a)) shows an ejection with horizontal-tail fins installed. The large positive pitch amplitudes obtained in the previous tests were reduced, and the store remained in a near level flight attitude during the entire time that the store was in the tunnel airstream.

Data showing a variation in prototype dynamic pressure (q_p) of the weapons pod are shown in figure 18(b) (tests 10 and 11). Test 7 has been repeated for comparison. It was found that varying q_p did not reduce the large positive pitch amplitudes obtained previously. However, the time to reach a particular pitch amplitude became larger as q_p was increased.

Pylon Tank Ejections

Photographs of the pylon tank ejections along with simulated conditions are shown in figure 13. The measured data are shown in figure 19. The ejection force was applied on the pylon tank in front of the center-of-gravity location by $x_s/d_s = 0.5819$.

The pylon tank at low altitude experienced large negative pitch angles in the immediate vicinity of the airplane model (test 12, fig. 19), which caused the tail of the tank to remain close to the trailing edge of the wing for approximately 25 milliseconds (model scale). Test 13 (fig. 19) shows a clean separation of the pylon tank at high altitude.

Tip Tank Ejections

Clean separation was obtained with an empty tip tank condition as shown in the photographs of figure 14. The measured data (fig. 20) indicate the yaw attitude angle (ψ_s) remained near 0° for approximately 20 milliseconds (model scale) after release (test 14). The pitch angle (θ_s) remained below -10° for approximately 25 milliseconds (model scale) after release. Test 15 (fig. 20) is a repeat of test 14, and shows a small change in the trajectories measured in the vertical plane. This change is attributed to not obtaining the same ejection energy in both tests.

Pylon Ejections

Photographs of the pylon ejections are shown in figure 15. The pylon appears to follow a downward trajectory while immersed in the tunnel airstream. However, erratic motions were experienced by the pylon after release, but did not come in contact with the airplane model.

Due to the erratic motions after release, no pylon trajectories or pitch amplitudes were measured.

Lateral Deviation and Angle of Yaw

As stated previously, the bottom view photographs are presented for the purpose of showing lateral deviation and angle of yaw. In general, it appears that lateral deviation and angle of yaw were not excessive while the stores tested were immersed in the tunnel airstream.

CONCLUSIONS

An investigation has been conducted in the 27- by 27-inch preflight jet facility at the NASA Wallops Station to determine the capability of a current fighter airplane to eject external stores at transonic and supersonic speeds.

The following results are indicated:

1. Satisfactory release characteristics were obtained with bomb 1 at a free-stream Mach number of 1.98 and high altitude.

2. Satisfactory release characteristics were obtained with bomb 2 at high subsonic speeds and low altitudes.

3. Unsatisfactory releases were obtained with the basic weapons pod configuration. However, by the addition of horizontal-tail fins, a satisfactory release was obtained at a free-stream Mach number of 1.39 and high altitude.

4. Clean separation was obtained with an empty pylon tank at a free-stream Mach number of 1.39 and high altitude. At low altitude the pylon tank experienced large negative pitch angles in the immediate vicinity of the airplane model. This caused the tail section of the tank to remain close to the wing trailing edge for approximately 25 milliseconds (model scale) after release.

5. Clean separation was obtained with an empty wing-tip tank at a free-stream Mach number of 1.39 and 11,000 feet.

6. Clean pylon separation was obtained at high subsonic and supersonic speeds, and at low and high altitudes, respectively. After release the pylon experienced erratic motions, but at no time came in contact with the airplane model.

7. In general, lateral deviation and angle of yaw did not appear excessive for the stores tested.

Langley Research Center,
National Aeronautics and Space Administration,
Langley Field, Va., July 27, 1959.

APPENDIX A

EJECTION ENERGY RELATIONSHIP

Since an ejection force (electric squibs) is used to eject the externally carried full-scale stores from the fighter configuration presented herein, it is necessary to scale the ejection energies in a manner similar to the dynamic scaling of the stores. Therefore, using some of the similarity relationships of reference 1 and the familar equation $F = Ma$, an expression for the model ejection energy is derived.

Modified Light Model Method

The ejection energy equations for the modified light model method are derived as follows:

$$\frac{F_M}{F_P} = \frac{m_M a_M}{m_P a_P} = \frac{w_M}{w_P}\frac{L_P}{L_M} = \frac{w_M}{w_P}\lambda^{-1}$$

$$\frac{E_M}{E_P} = \frac{F_M}{F_P}\frac{S_M}{S_P} = \frac{F_M}{F_P}\lambda$$

$$\frac{E_M}{E_P} = \frac{w_M}{w_P}$$

From reference 1

$$w_M = w_P \frac{p_M}{p_P}\lambda^3$$

therefore

$$E_M = E_P \lambda^3 \frac{p_M}{p_P}$$

Heavy Model Method

The ejection energy equations for the heavy model method are derived as follows:

$$\frac{F_M}{F_P} = \frac{m_M a_M}{m_P a_P}$$

$$a_M = a_P \quad \text{(ref. 1)}$$

$$\frac{F_M}{F_P} = \frac{w_M/g}{w_P/g} = \frac{w_M}{w_P}$$

$$\frac{F_M}{F_P} = \frac{p_M}{p_P} \lambda^2$$

From reference 1

$$w_M = w_P \frac{p_M}{p_P} \lambda^2$$

$$\lambda \frac{F_M}{F_P} = \frac{E_M}{E_P} \quad \text{(from above)}$$

therefore

$$E_M = E_P \frac{p_M}{p_P} \lambda^3$$

Therefore, the model ejection energy is independent of the method of simulation.

REFERENCE

1. Sandahl, Carl A., and Faget, Maxime A.: Similitude Relations for Free-Model Wind-Tunnel Studies of Store-Dropping Problems. NACA TN 3907, 1957.

TABLE I.- SUMMARY OF TEST DATA

Run No.	Test No.	Mach No.	a_M, initial g units	h_a, initial ft	wt, lb	$I_{y,M}$ slug-ft^2	α_w, deg	Δt, msec	q_∞, lb/ft^2	Store	Scaling method	Remarks
1,875	1	1.98	6.28	26,370	6.12	0.01458	1	13.34 6.67	6,100	Bomb 1	H-M	Airplane model accelerated upward to compensate for weight deficiency
1,876	2	1.98	5.20	22,100	6.12	0.01458	1	13.34 6.67	6,070	Bomb 1	H-M	Repeat of test 1
1,877	3	1.98	1.95	20,000	6.18	0.01458	0.6	13.34 6.67	6,120	Bomb 1	H-M	Airplane model accelerated upward to compensate for weight deficiency
1,878	4	1.98	2.72	27,750	6.18	0.01458	0.6	13.34 6.67	6,070	Bomb 1	H-M	Repeat of test 3
1,890	5	0.897	2.59	7,550	5.28	0.01153	1.5	19.84 9.92	1,230	Bomb 2	H-M	Horizontal fins only, airplane model accelerated to compensate for weight deficiency
1,891	6	0.915	2.95	10,875	5.28	0.01153	1.5	18.00 9.00	1,260	Bomb 2	H-M	Same as test 5
2,016	7	1.39	6.5	33,750	2.02	0.00436	2	8.20 4.10	2,870	Weapons pod	M-IM	
2,017	8	1.39	5.98	33,670	2.07	0.00514	2	8.34 4.17	2,915	Weapons pod	M-IM	Horizontal-tail fins installed
2,018	9	1.39	5.55	31,820	2.05	0.00461	2	8.38 4.19	2,860	Weapons pod	M-IM	Weight added to move c.g. aft
2,014	10	1.39	4.69	27,600	2.02	0.00436	2	8.5 4.25	3,010	Weapons pod	M-IM	q_p test
2,015	11	1.39	5.44	30,500	2.02	0.00436	2	8.36 4.18	2,960	Weapons pod	M-IM	q_p test
1,751	12	1.39	0	7,800	1.673	0.00522	1.5	5.04	3,035	Empty pylon tank	H-M	Reinforced plastic construction
1,756	13	1.39	0	40,000	6.77	0.02110	3.5	5.08	3,139	Empty pylon tank	H-M	Reinforced plastic construction
1,886	14	1.39	0	11,000	2.27	0.01437	1.5	16.68 8.34	3,125	Empty tip tank	H-M	
1,887	15	1.39	0	11,000	2.27	0.01437	1.5	16.68 8.34	3,085	Empty tip tank	H-M	Repeat of test 14
1,892	16	0.86	0	Sea level	0.599	4.36×10^{-4}	6.0	4.00 2.00	1,125	Pylon	H-M	
1,893	17	0.85	0	Sea level	0.599	4.36×10^{-4}	6.0	4.00 2.00	1,100	Pylon	H-M	Repeat of test 16
1,732	18	1.39	10.60	39,900	0.406	2.74×10^{-4}	3.5	5.10	3,140	Pylon	M-IM	
1,733	19	1.39	10.92	8,400	0.1005	6.78×10^{-5}	1.5	2.35	2,988	Pylon	M-IM	
1,780	20	1.98	9.64	37,900	0.406	2.74×10^{-4}	1.5	0.771	6,075	Pylon	M-IM	
1,883	21	1.98	3.00	24,700	0.584	4.36×10^{-4}	1.0	1.428 .714	6,230	Pylon	H-M	Airplane model accelerated upward to compensate for weight deficiency

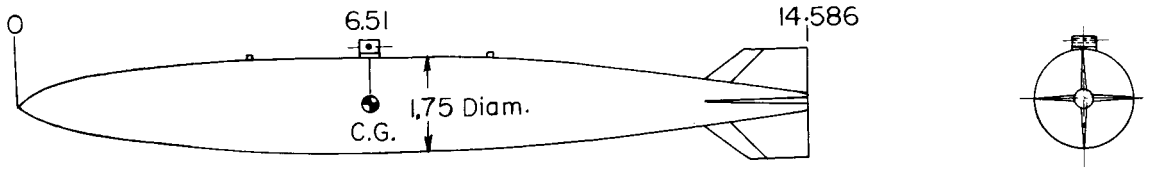

(a) Bomb 1; $l_s/d_s = 8.33$.

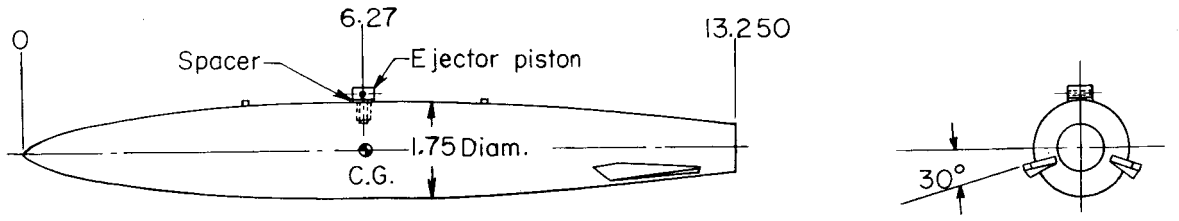

(b) Bomb 2; $l_s/d_s = 7.57$.

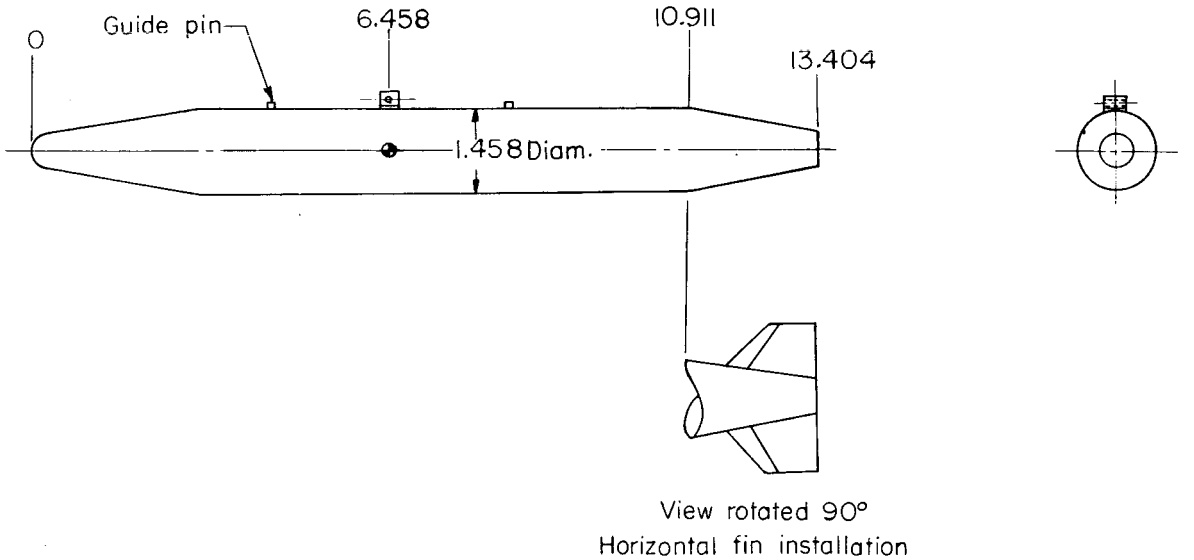

(c) Weapons pod; $l_s/d_s = 9.20$.

Figure 1.- The 0.0858-scale models of externally carried fuselage stores. All dimensions are in inches.

[redacted]

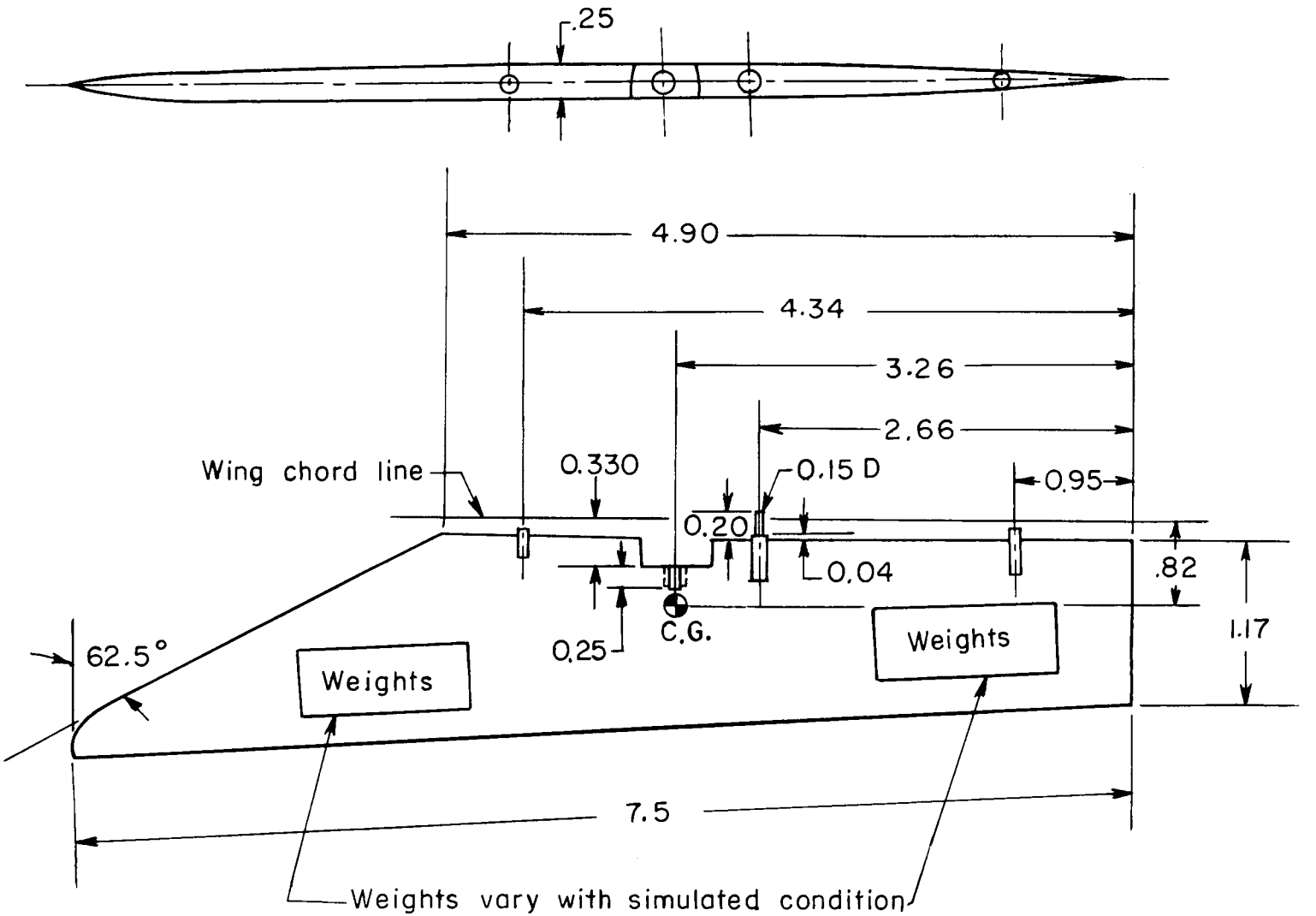

Figure 2.- The 0.0858-scaled model of wing pylon. All dimensions are in inches.

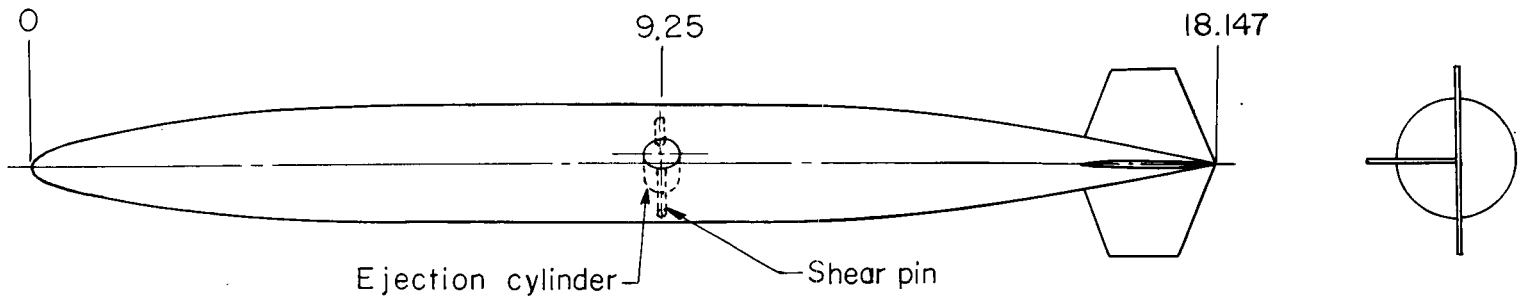

View rotated 90° from ejection plane.

Top view

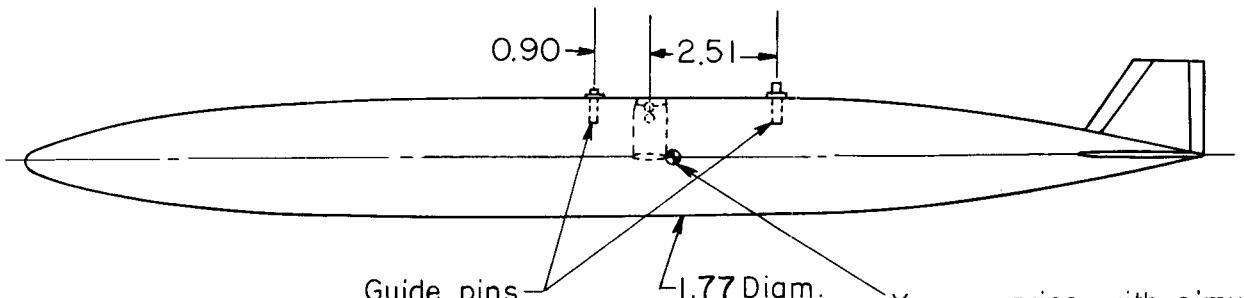

Side view

Figure 3.- The 0.0858-scaled model of pylon mounted fuel tank. All dimensions are in inches. $l_s/d_s = 10.25$.

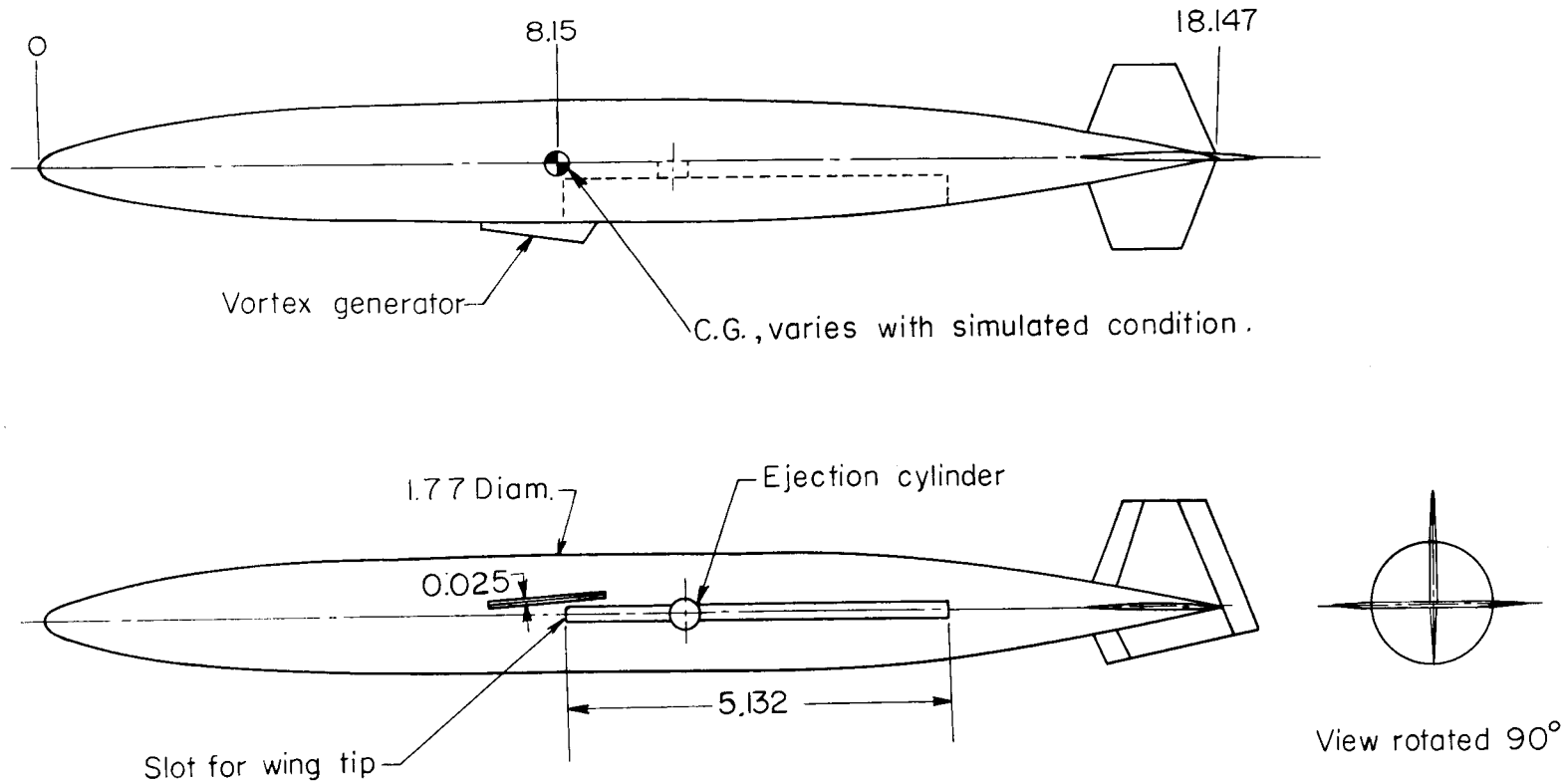

Figure 4.- The 0.0858-scaled model of wing-tip tank. All dimensions are in inches. $l_s/d_s = 10.25$.

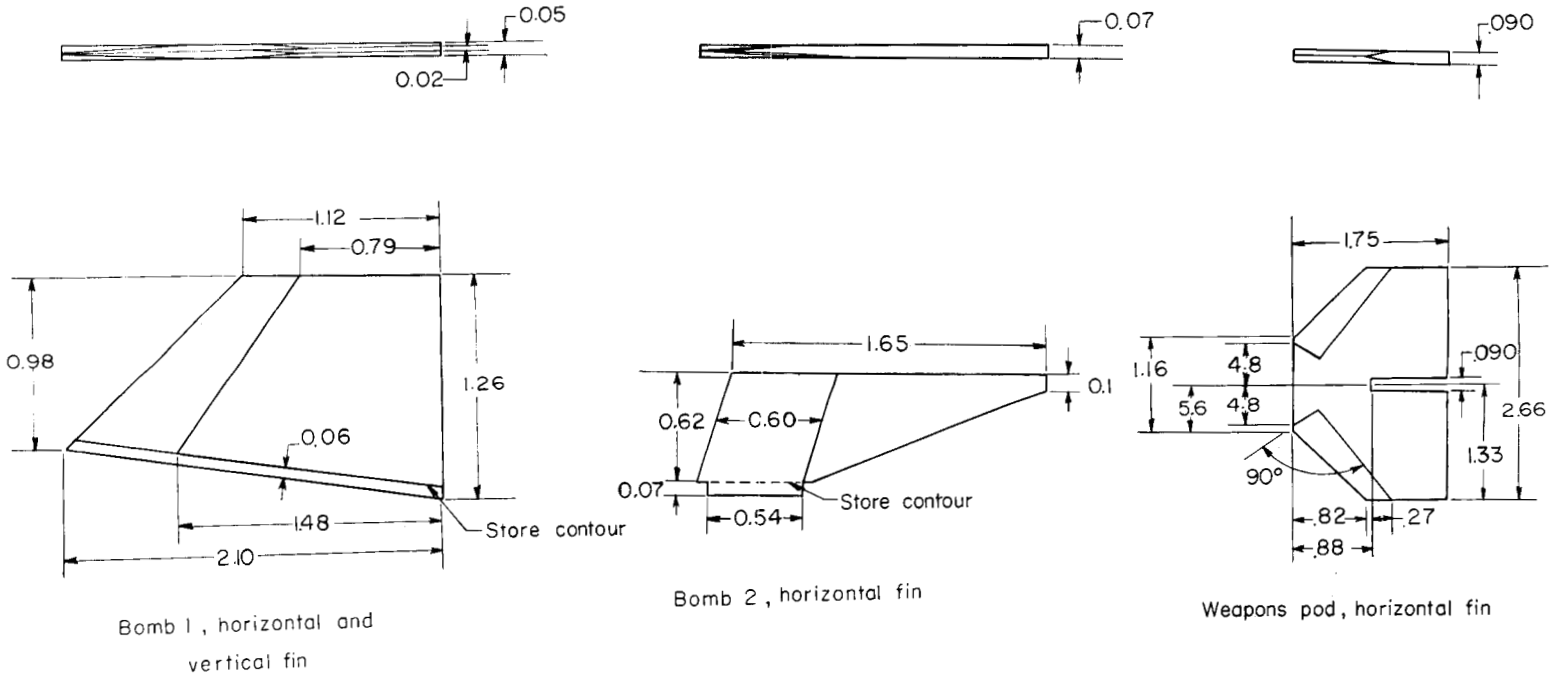

Figure 5.- Fin dimensions and designations for fuselage stores. All dimensions are in inches.

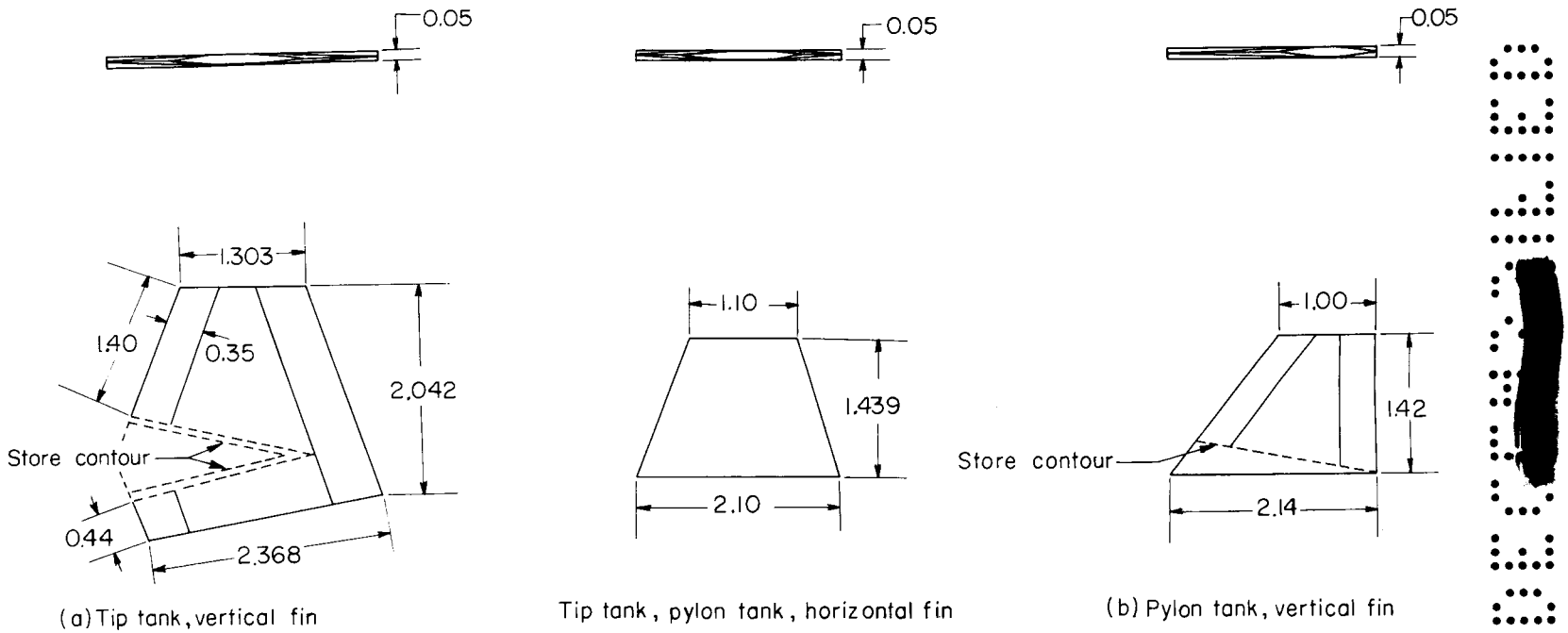

Figure 6.- Dimensions and details of pylon and tip tank store fins. All dimensions are in inches.

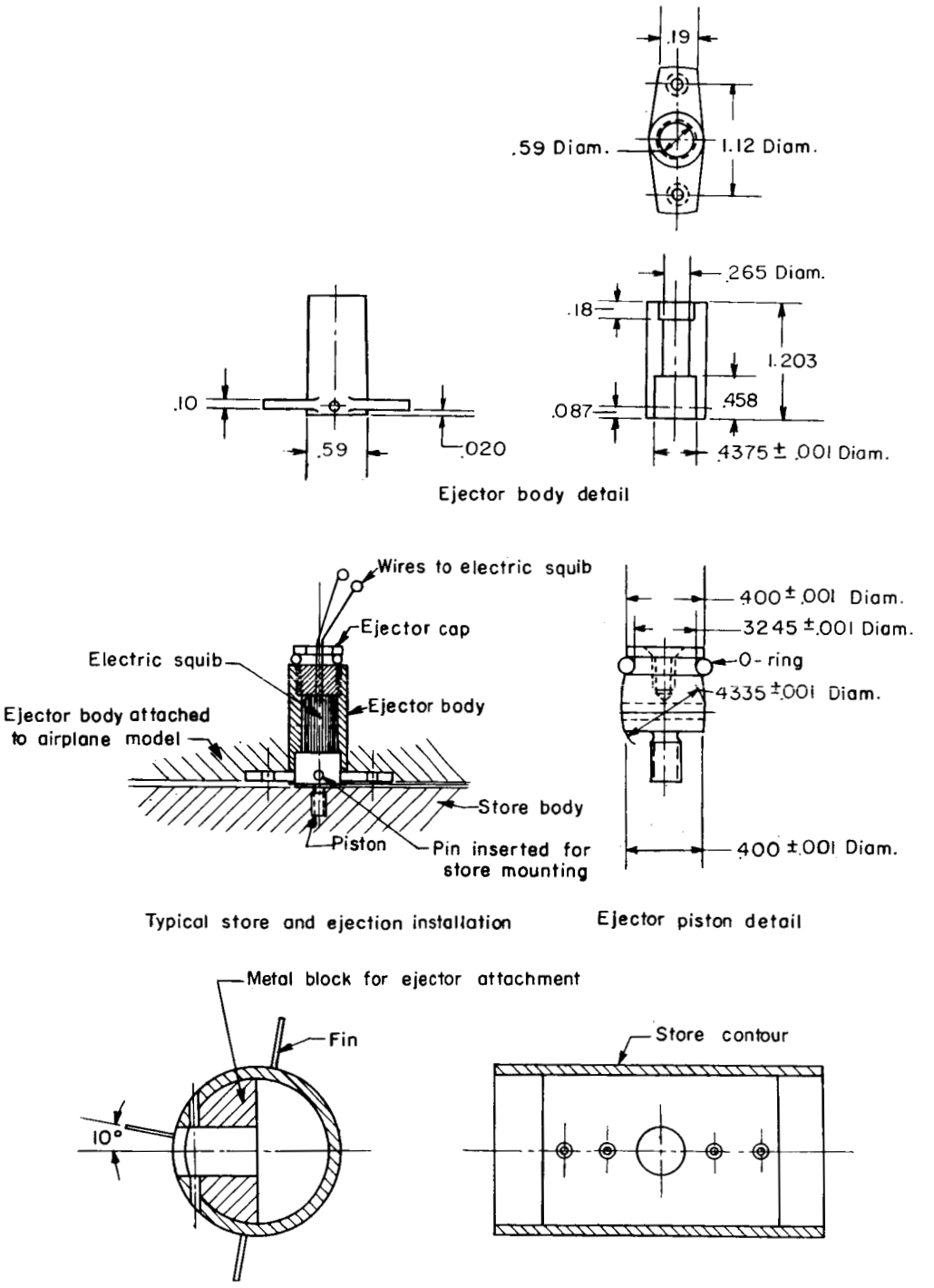

Figure 7.- Typical ejector detail. All dimensions are in inches.

L-545

[redacted]

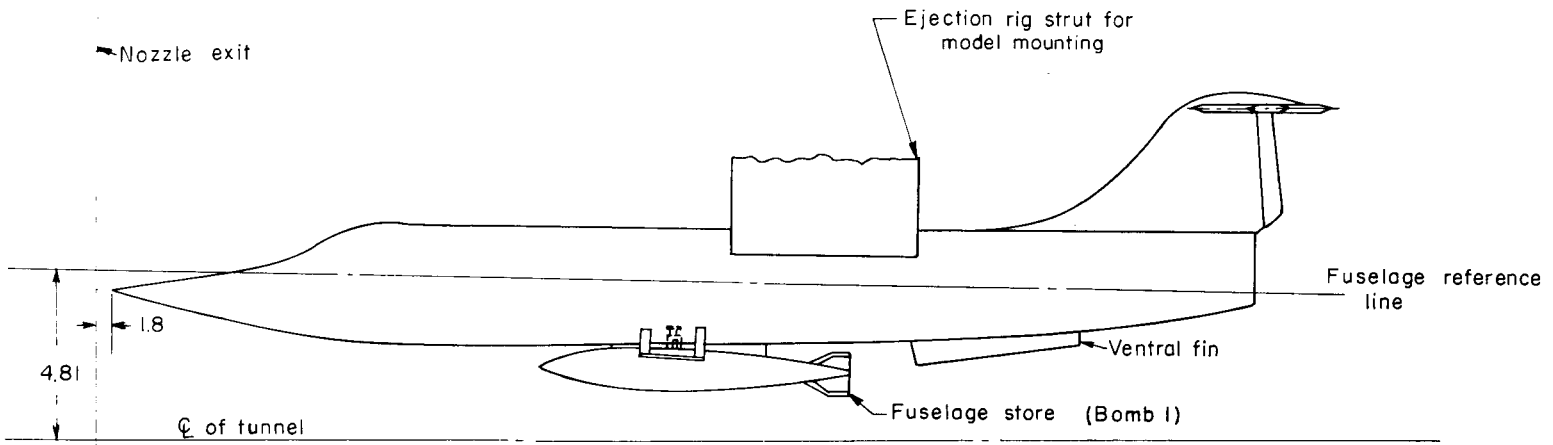

(a) Side view.

Figure 8.- The 0.0858-scaled model of a current fighter airplane in preflight test facility. All dimensions are in inches.

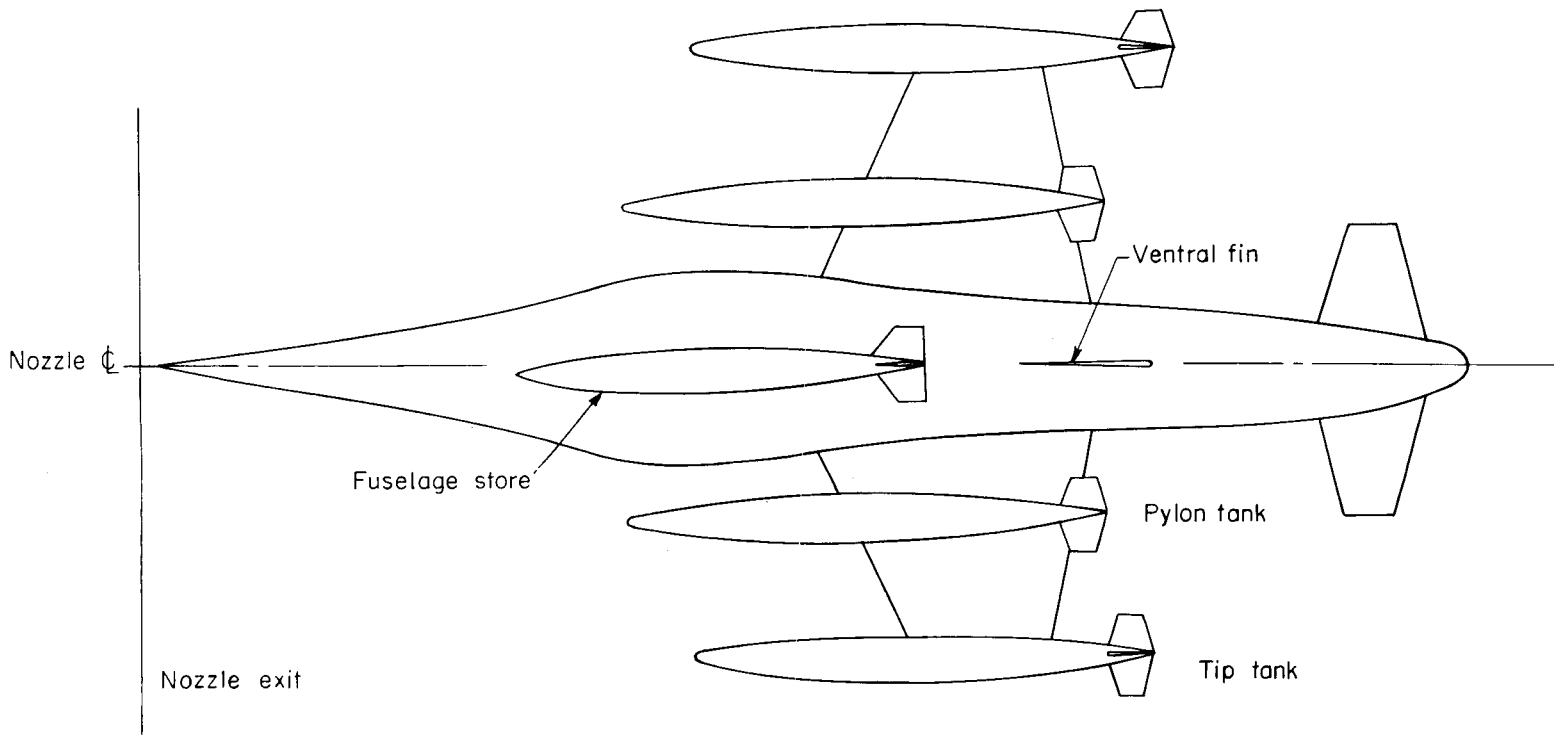

(b) Bottom view.

Figure 8.- Concluded.

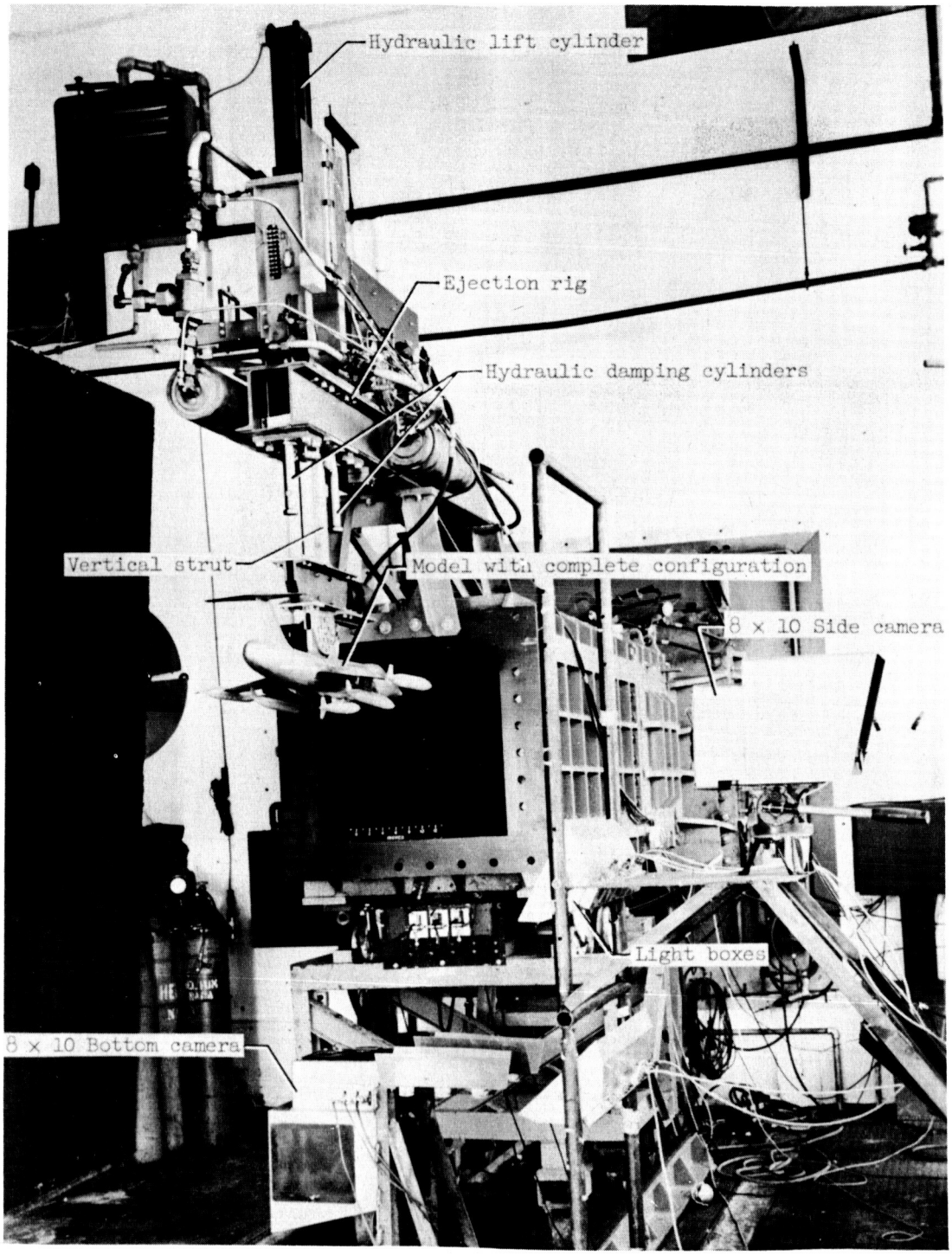

L-57-5636.1

Figure 9.- Equipment installation in the 27- by 27-inch preflight jet.

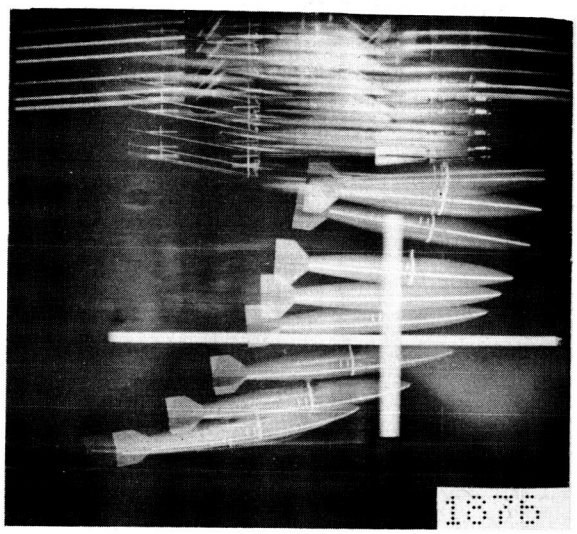

Test 2; side view

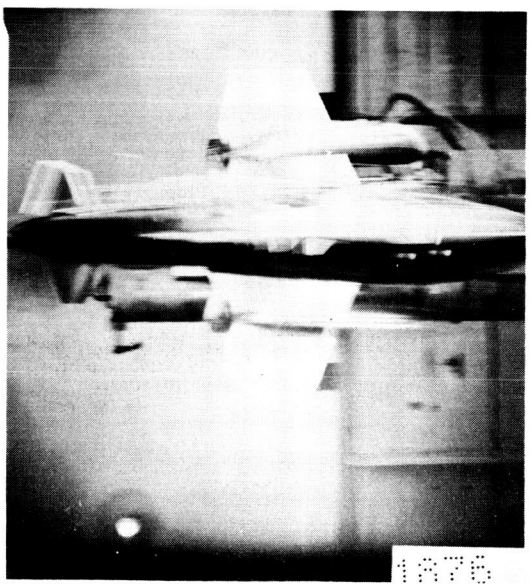

Test 2; bottom view; repeat of test 1; h_a = 22,100 feet

(b) Test 2.

L-59-5019

Figure 10.- Continued.

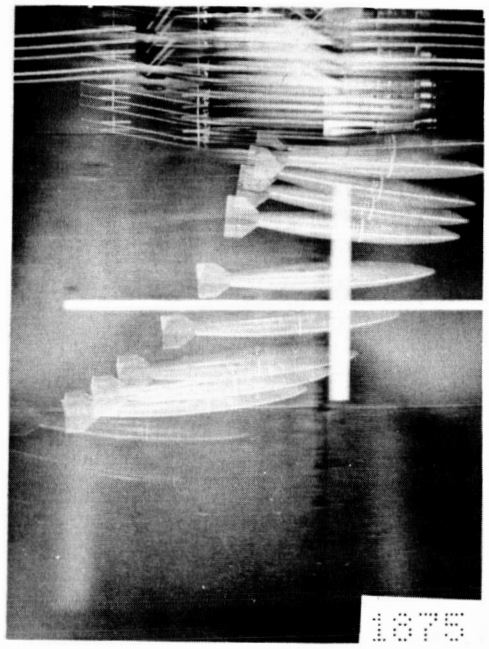

Test 1; side view

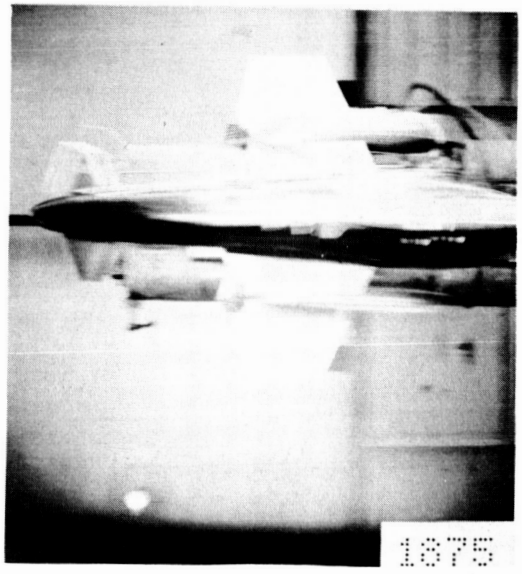

Test 1; bottom view; h_a = 26,370 feet ; α_w = 1°

(a) Test 1. L-59-5018

Figure 10.- Microflash photographs of bomb 1 ejections. M_∞ = 1.98.

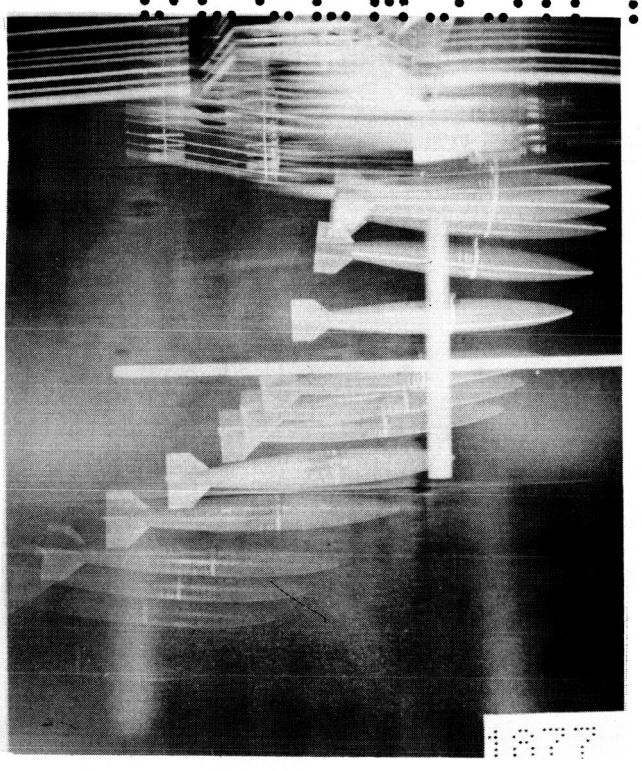

Test 3; side view

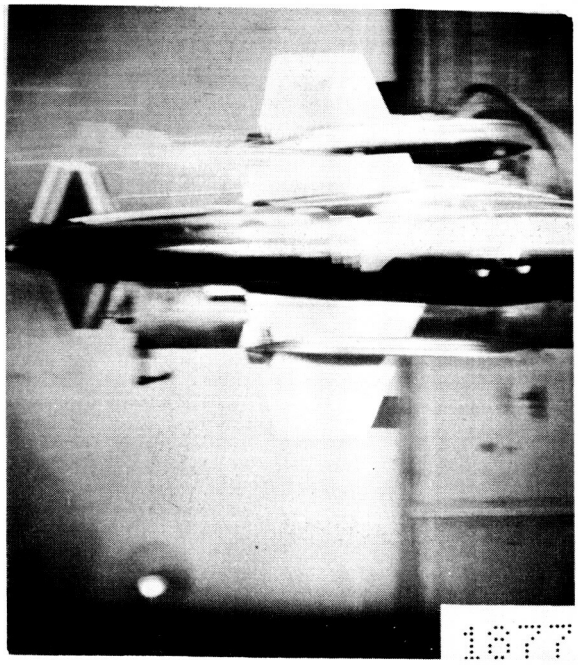

Test 3; bottom view; h_a = 20,000 feet; α_w=0.6°

(c) Test 3.

L-59-5020

Figure 10.- Continued.

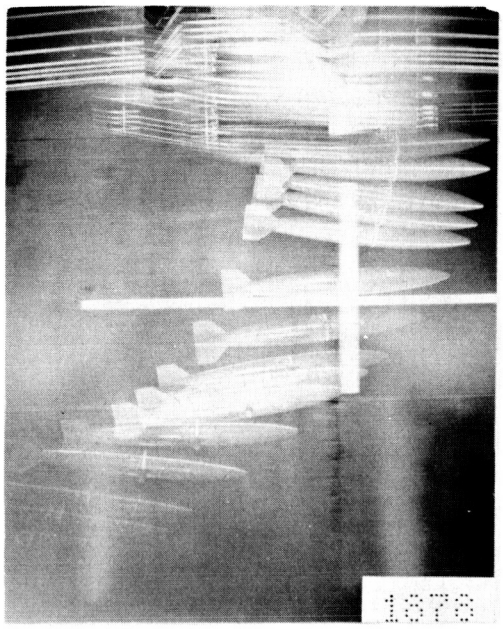

Test 4; side view

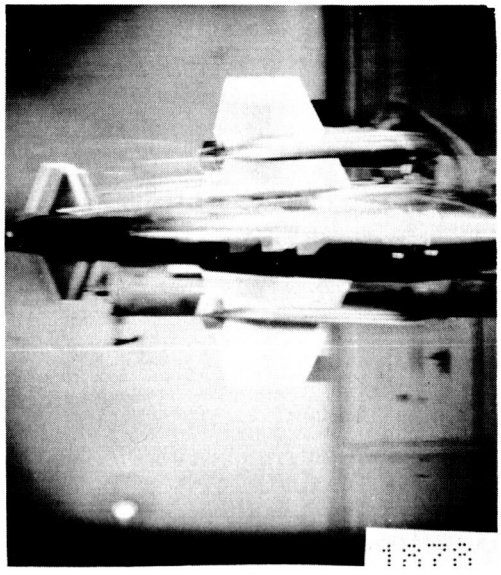

Test 4; bottom view; repeat of test 3; h_a = 27,750 feet

(d) Test 4.

L-59-5021

Figure 10.- Concluded.

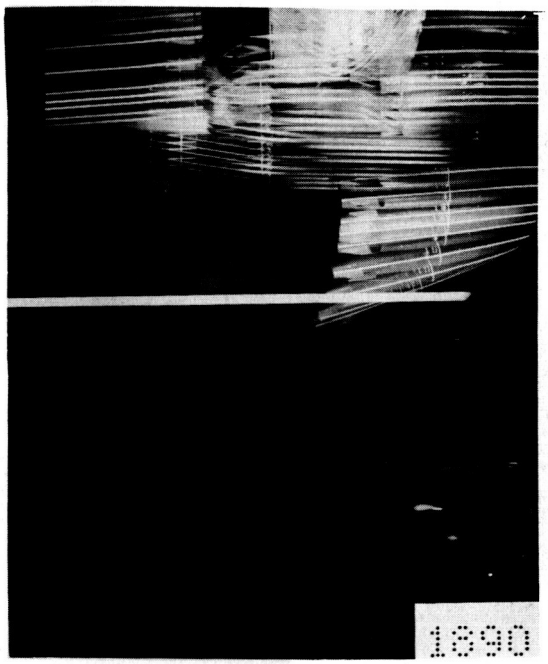

Test 5; side view

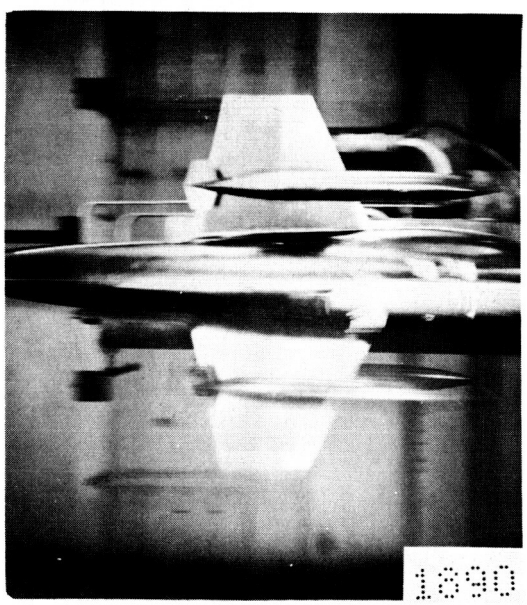

Test 5; bottom view; h_a = 7,550 feet

(a) Test 5.

L-59-5022

Figure 11.- Microflash photographs of bomb 2 ejections. M_∞ = 0.9; α_w = 1.5°.

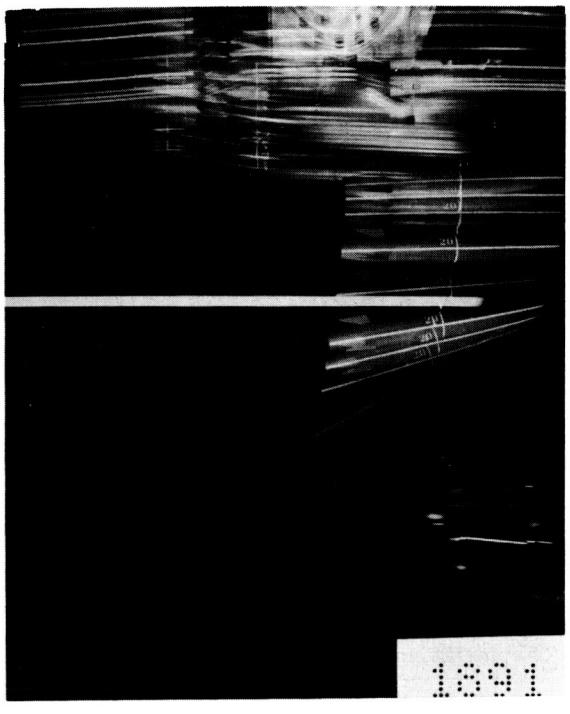

Test 6; side view

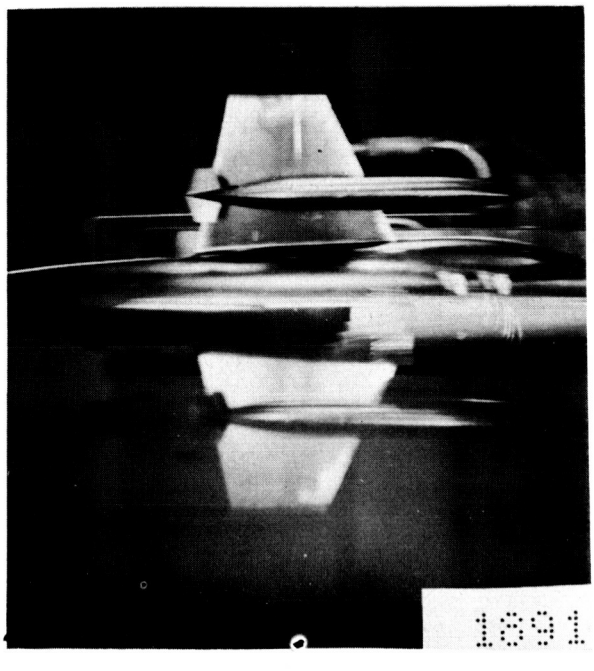

Test 6; bottom view; repeat of test 5 ; h_a = 10,875 feet

(b) Test 6.

L-59-5023

Figure 11.- Concluded.

L-545

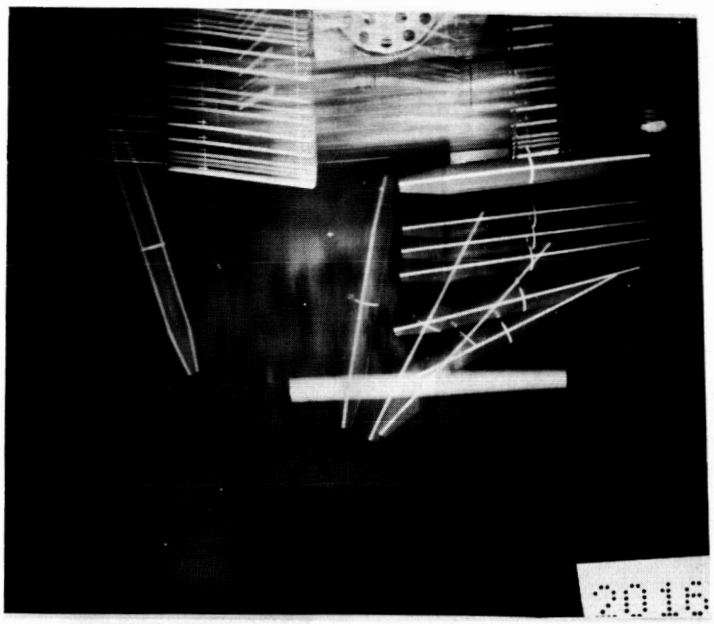

Test 7; side view

Test 7; bottom view; h_a = 33,750 feet; q_p = 730 lb/ft^2

(a) Test 7. L-59-5024

Figure 12.- Microflash photographs of weapons pod ejections. M_∞ = 1.39; α_w = 2°.

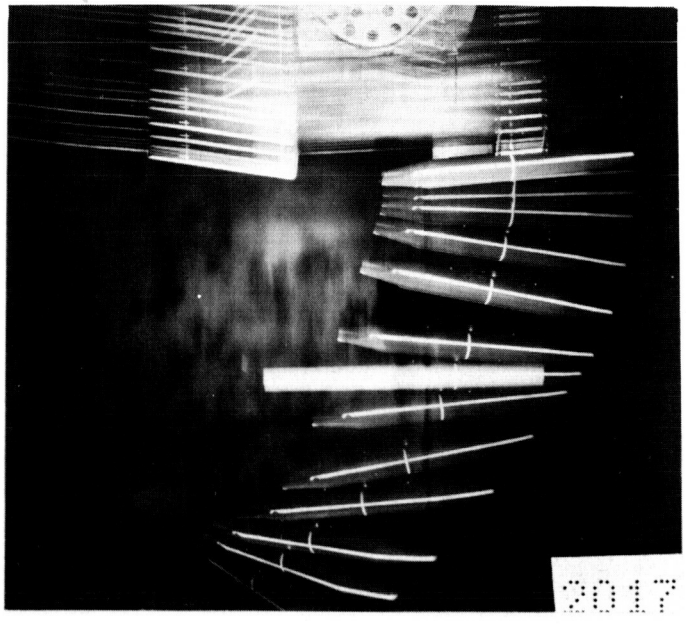

Test 8; side view

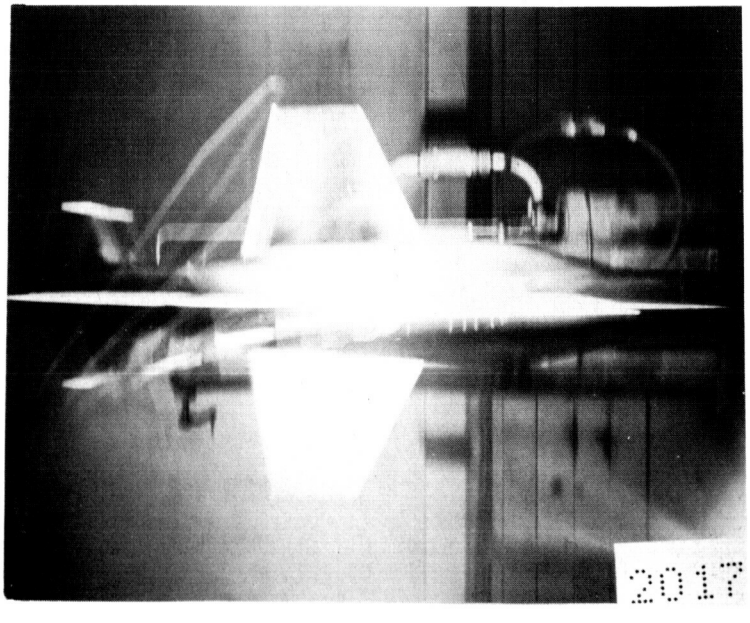

Test 8; bottom view; h_a = 33,670 feet; q_p = 725 lb/ft^2

(b) Test 8. L-59-5025

Figure 12.- Continued.

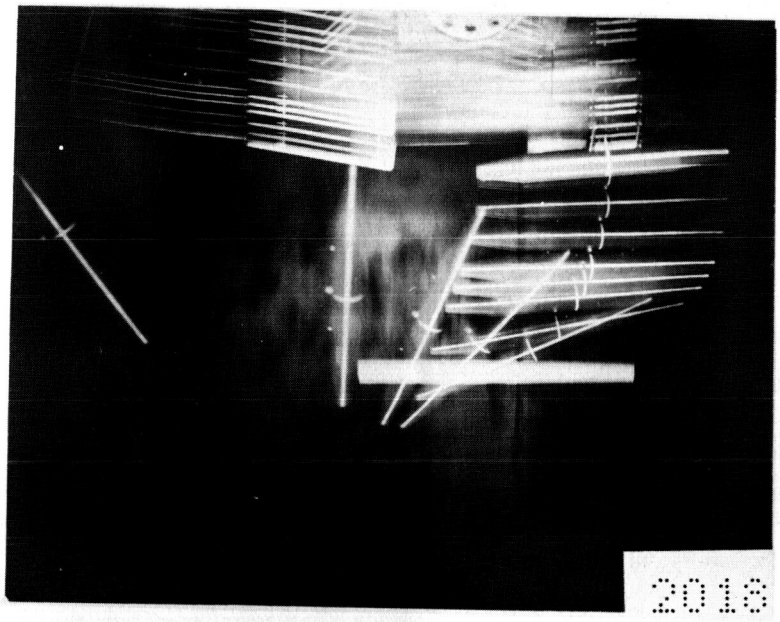

Test 9; side view

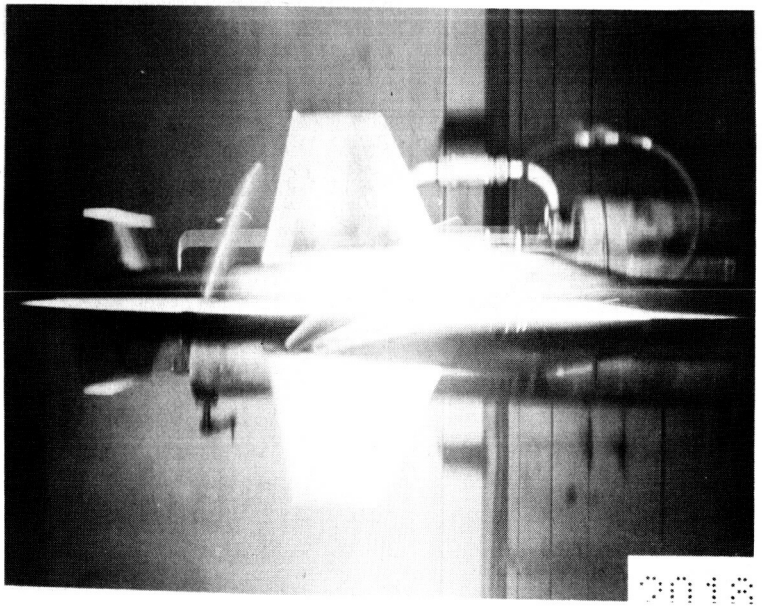

Test 9; bottom view; h_a = 31,820 feet; q_p = 795 lb/ft^2

(c) Test 9.

L-59-5026

Figure 12.- Continued.

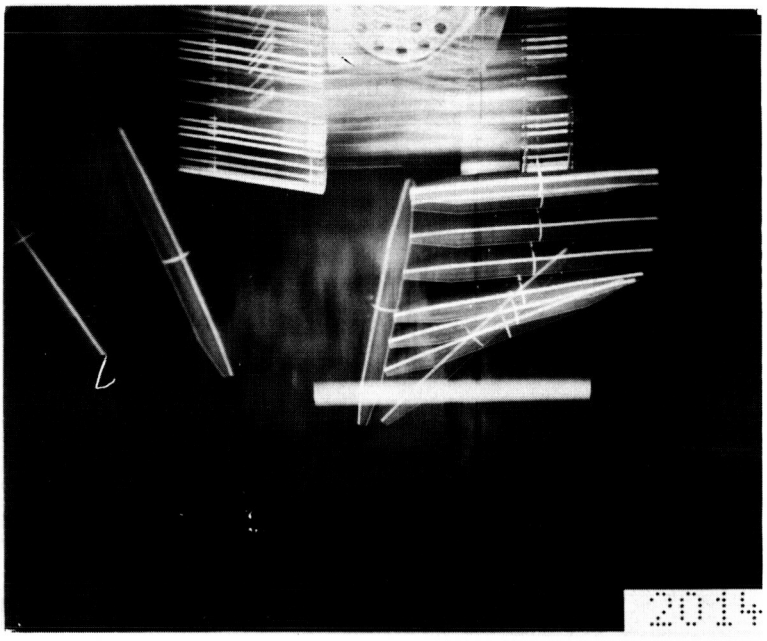

Test 10; side view

Test 10; bottom view; h_a =27,600 feet; q_p=950 lb/ft^2

(d) Test 10.

L-59-5027

Figure 12.- Continued.

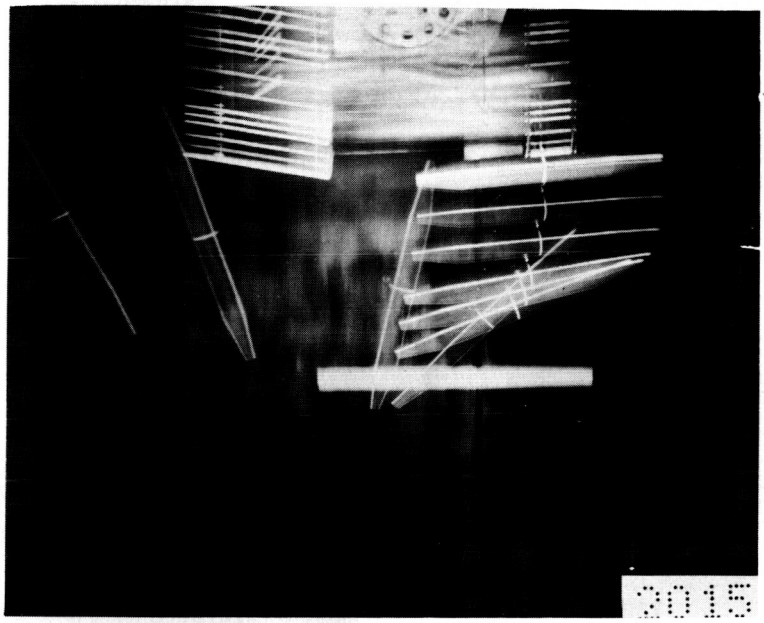

Test 11; side view

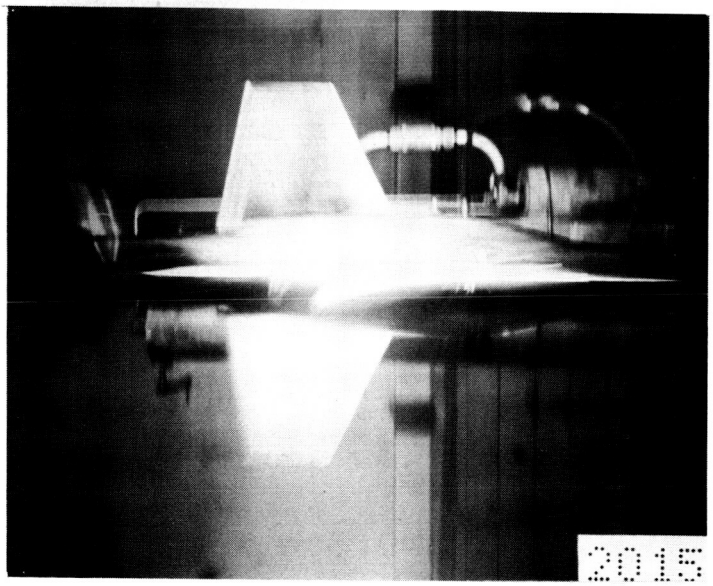

Test 11; bottom view; h_a = 30,500 feet; q_p = 850 lb/ft^2

(e) Test 11.

L-59-5028

Figure 12.- Concluded.

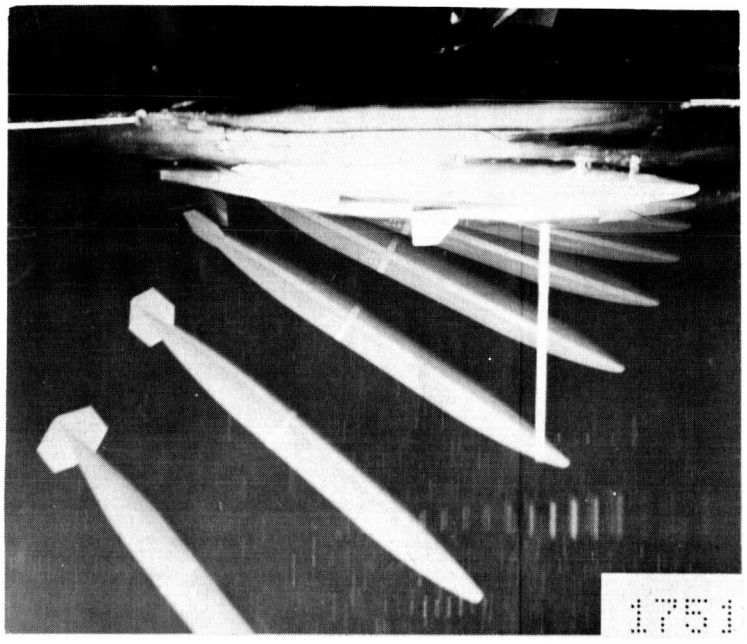

Test 12; side view

Test 12; bottom view; h_a = 7,800 ft; α_w = 1.5°

(a) Test 12.

L-59-5029

Figure 13.- Microflash photographs of pylon tank ejections. M_∞ = 1.39.

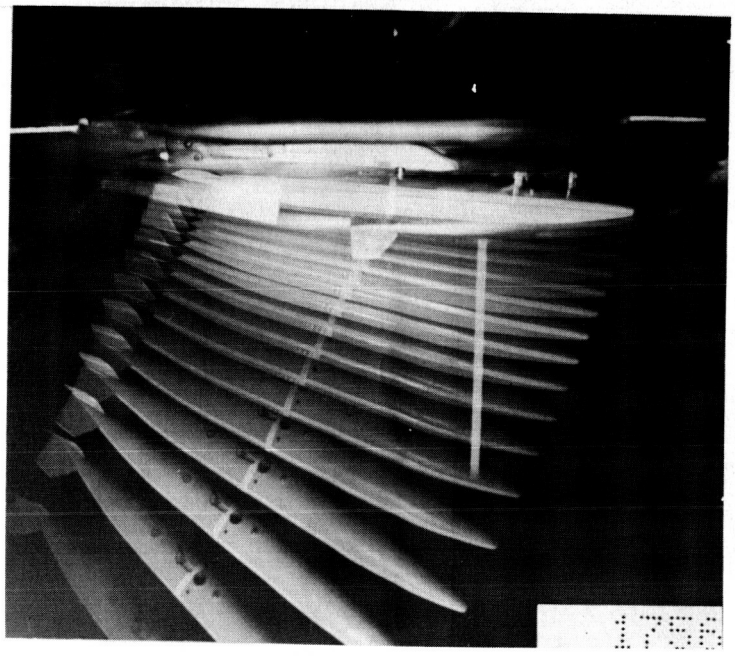

Test 13; side view

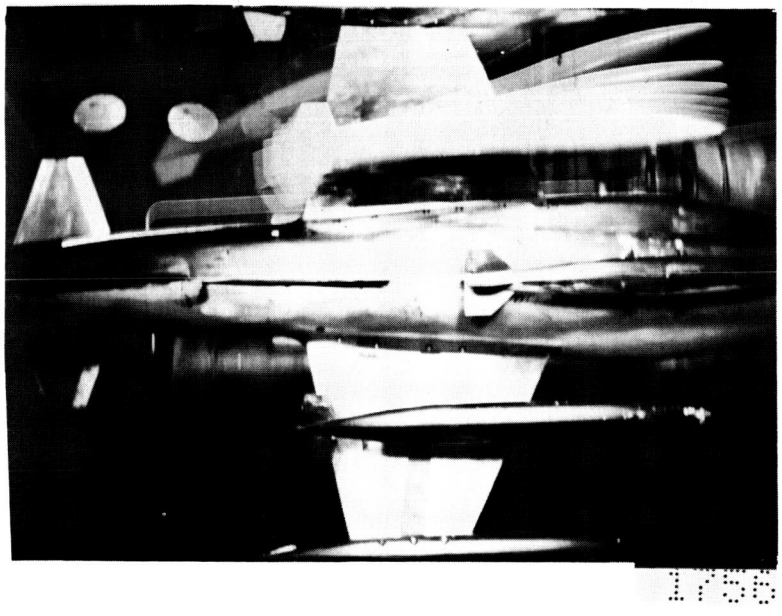

Test 13; bottom view; $h_a = 40,000$ feet; $\alpha_w = 3.5°$

(b) Test 13.

L-59-5030

Figure 13.- Concluded.

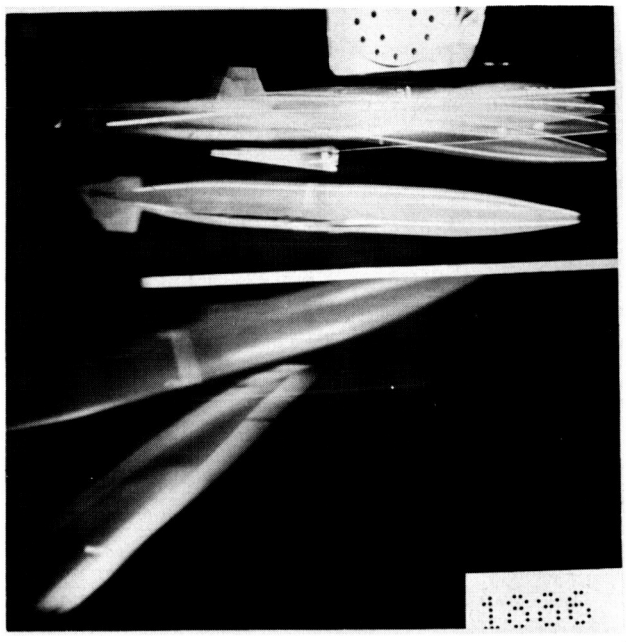

Test 14; side view

Test 14; bottom view

(a) Test 14. L-59-5031

Figure 14.- Microflash photographs of tip tank ejections. $M_\infty = 1.39$; $h_a = 11{,}000$ feet; $\alpha_w = 1.5^\circ$.

Test 15; side view

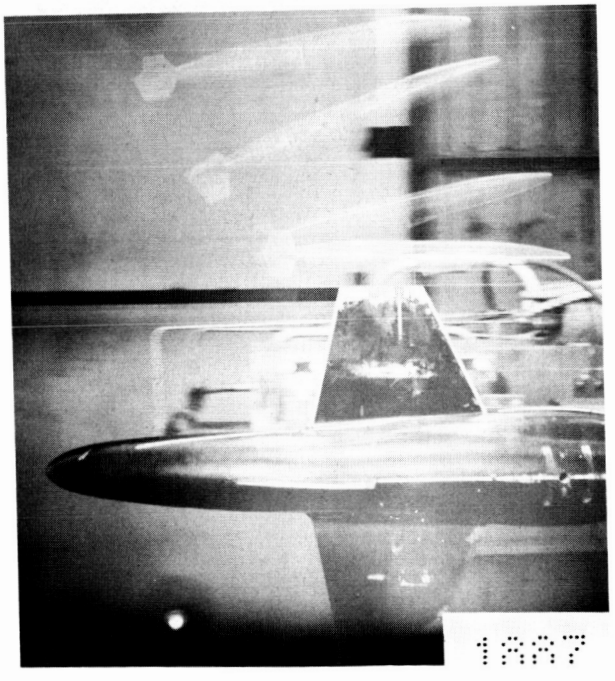

Test 15 ; bottom view; repeat of test 14

(b) Test 15.

L-59-5032

Figure 14.- Concluded.

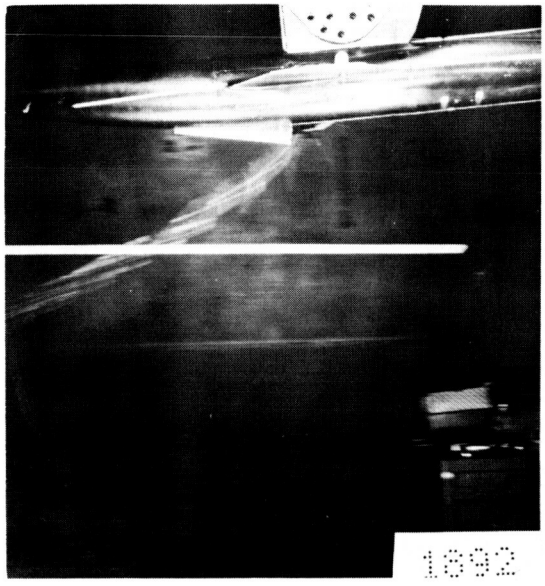

Test 16; side view

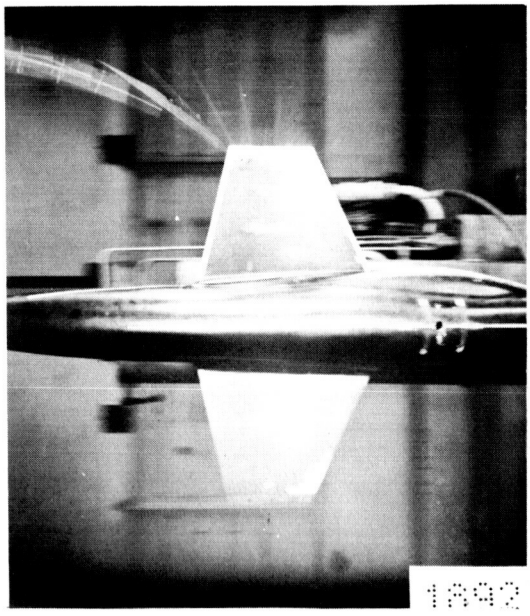

Test 16; bottom view; $M_\infty = .86$; h_a = sea level; $\alpha_w = 6°$

(a) Test 16.

L-59-5033

Figure 15.- Microflash photographs of pylon store ejections.

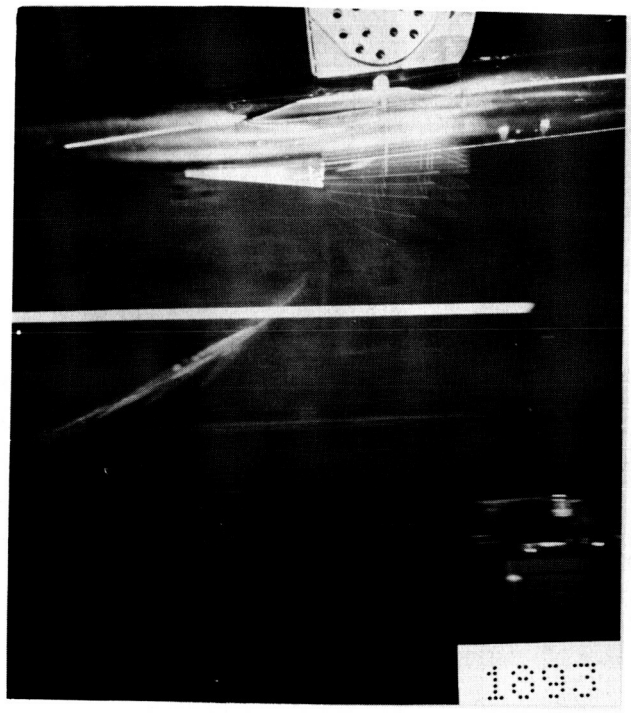

Test 17; side view

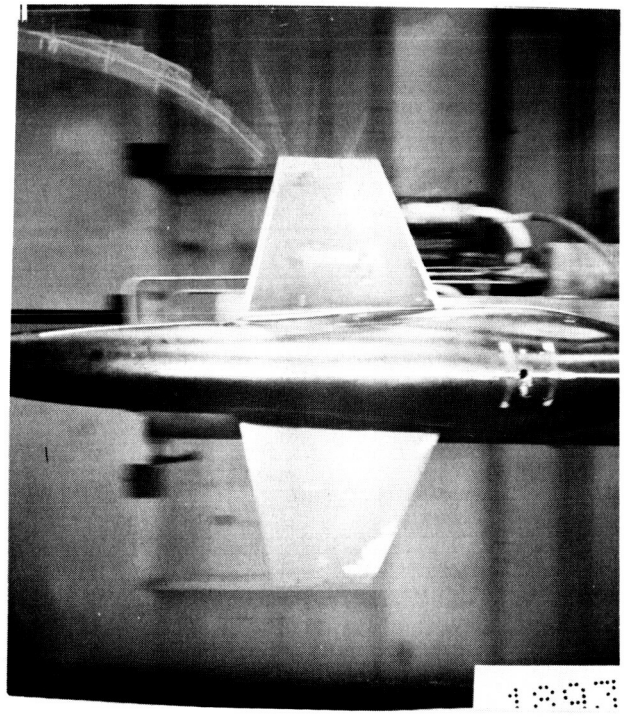

Test 17; bottom view; $M_\infty = .85$; h_a = sea level; $\alpha_w = 6°$

(b) Test 17.

L-59-5034

Figure 15.- Continued.

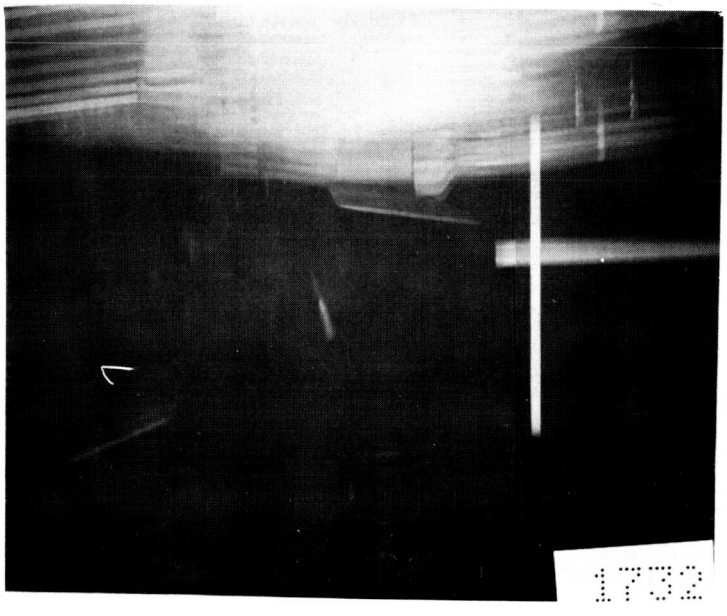

Test 18; side view

Test 18; bottom view; $M_\infty = 1.39$; $h_a = 39,900$ feet; $\alpha_w = 3.5°$

(c) Test 18.

L-59-5035

Figure 15.- Continued.

Test 19; side view

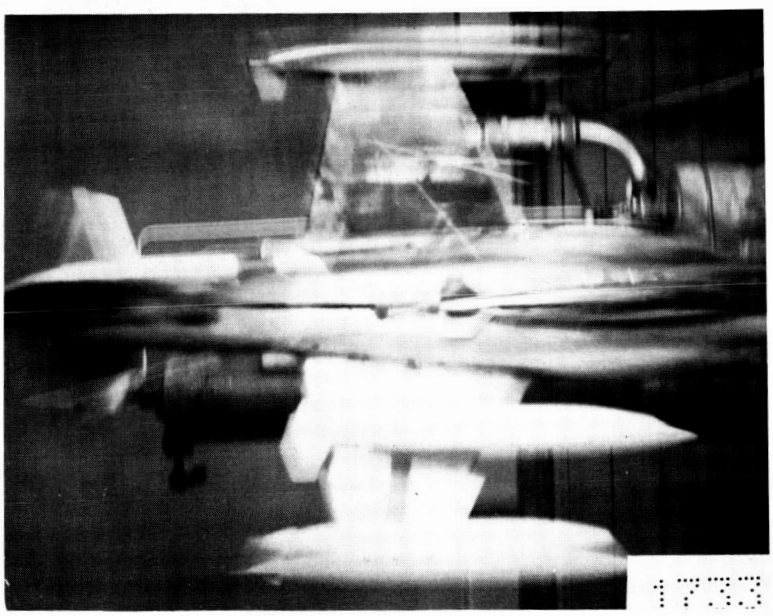

Test 19; bottom view; $M_\infty = 1.39$; $h_a = 8,400$; $\alpha_w = 1.5°$

(d) Test 19.

L-59-5036

Figure 15.- Continued.

Test 20; side view

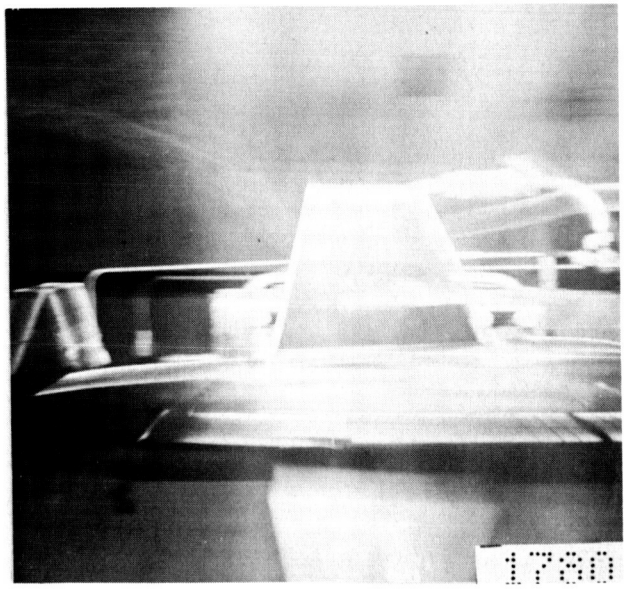

Test 20; bottom view; $M_\infty = 1.98$; $h_a = 37{,}900$ feet; $\alpha_w = 1.5°$

(e) Test 20. L-59-5037

Figure 15.- Continued.

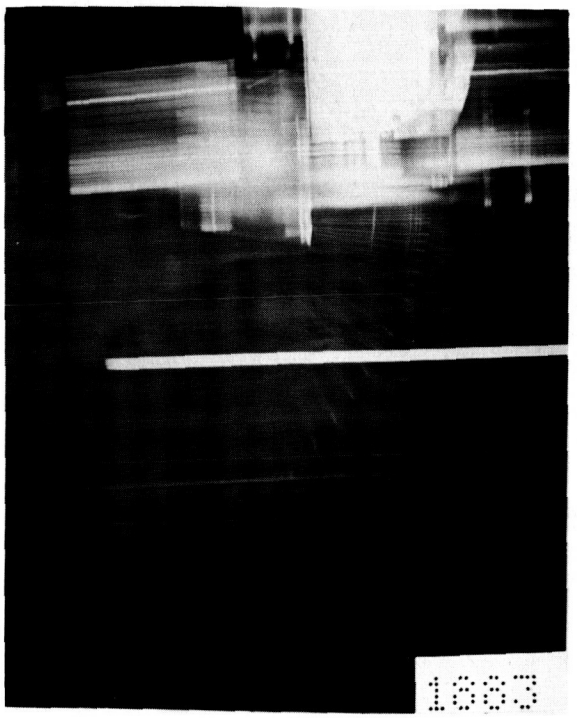

Test 21; side view

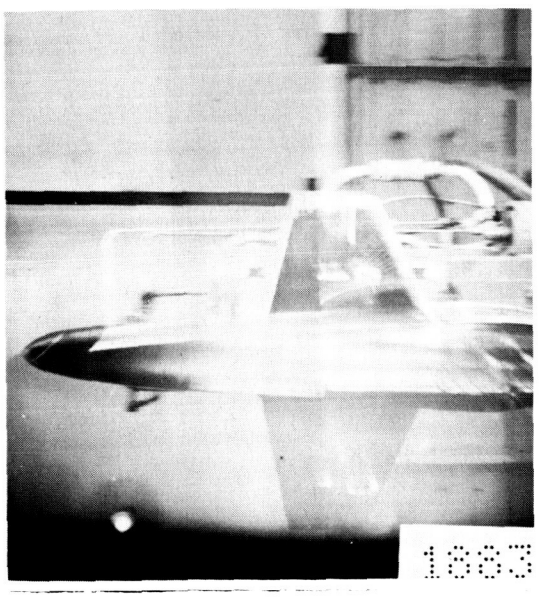

Test 21; bottom view; $M_\infty = 1.98$; $h_a = 24{,}700$ feet; $\alpha_w = 1°$

(f) Test 21.

L-59-5038

Figure 15.- Concluded.

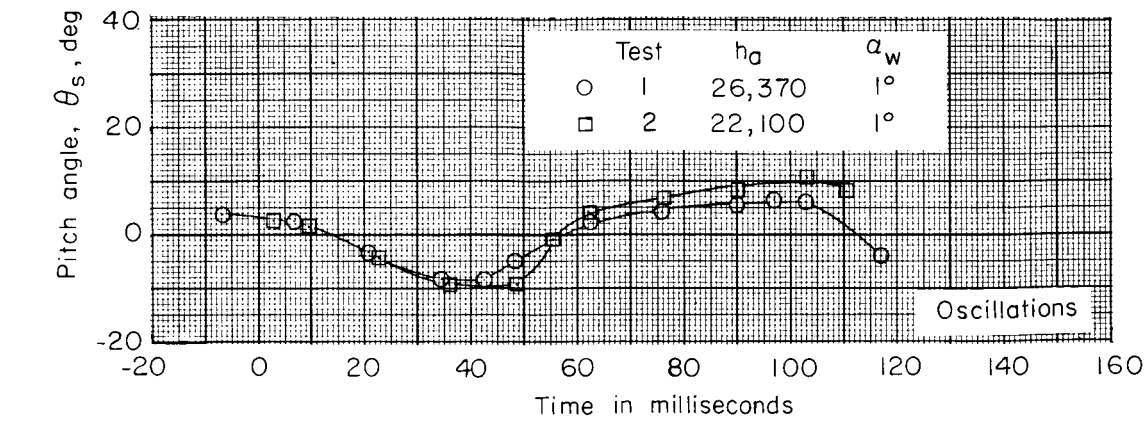

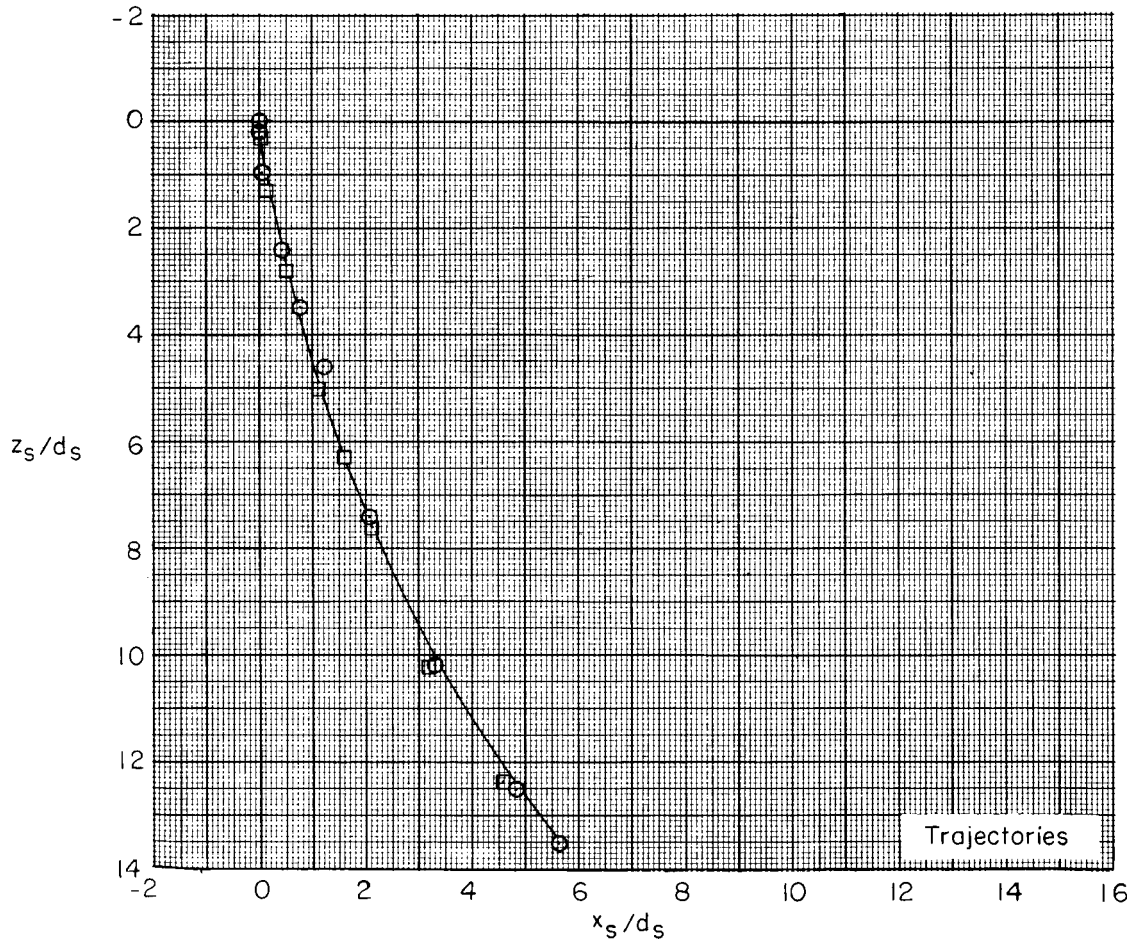

Figure 16.- Bomb 1 oscillations and trajectories at $M_\infty = 1.98$.

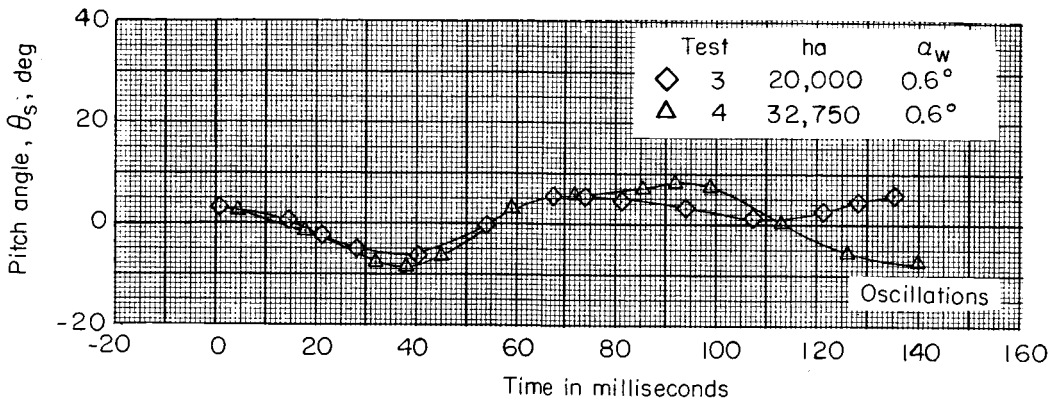

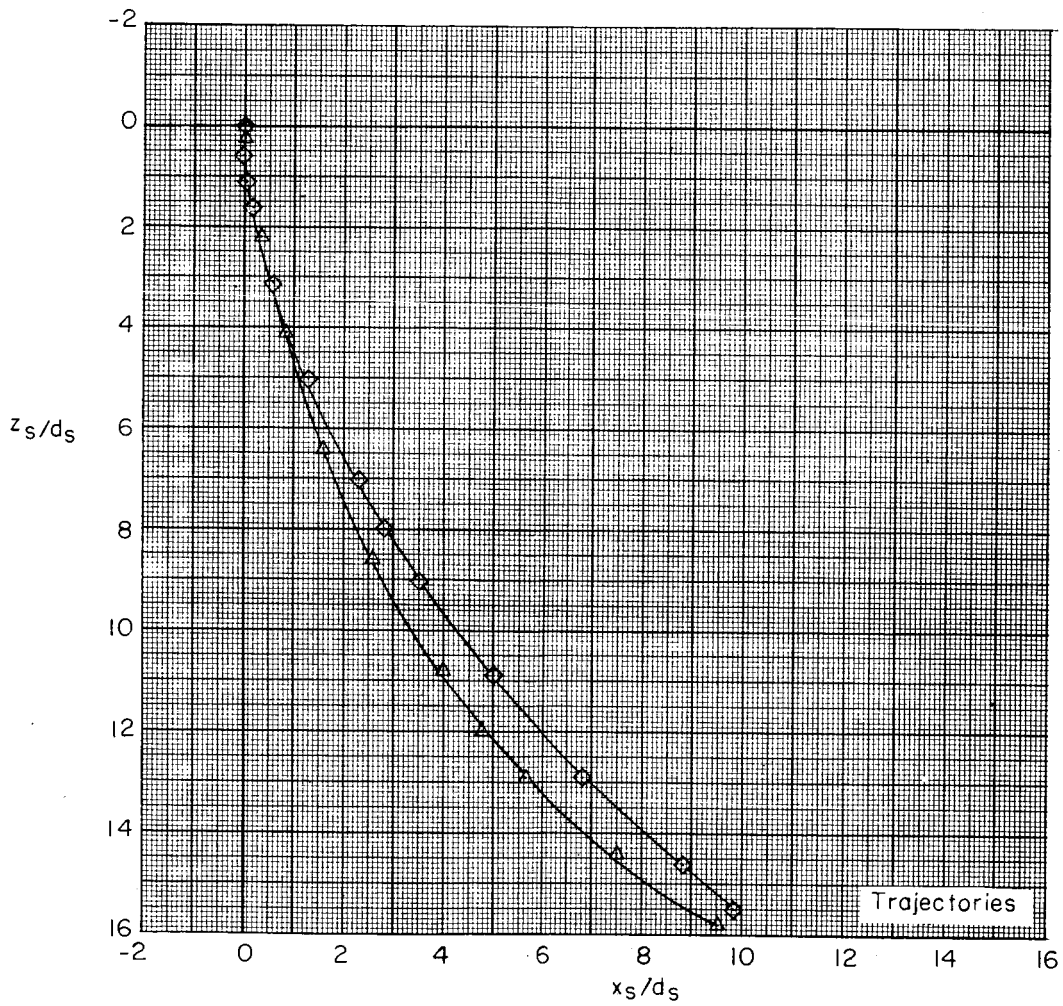

Figure 16.- Concluded.

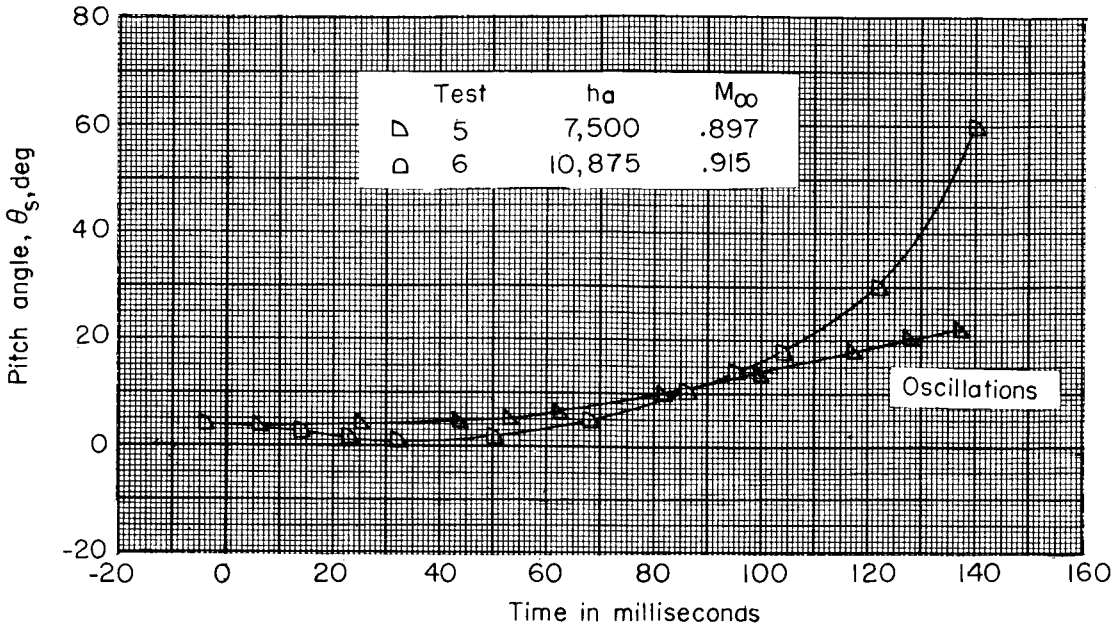

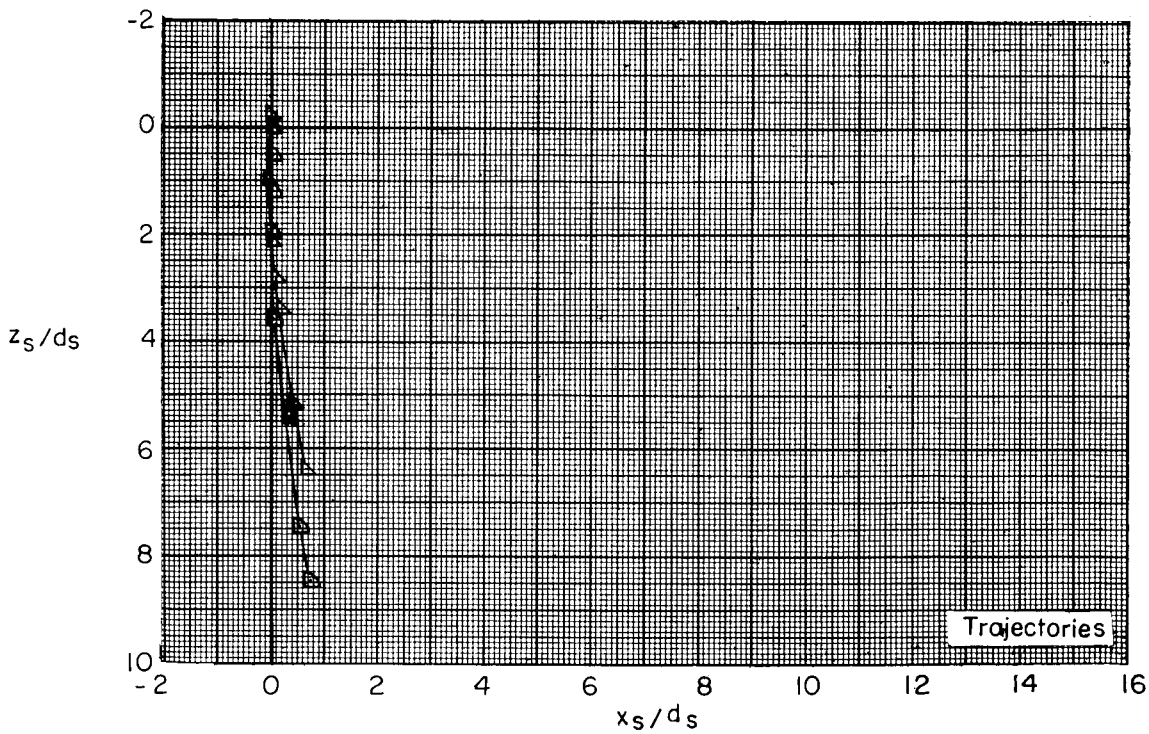

Figure 17.- Bomb 2 oscillations and trajectories. $\alpha_w = 1.5^\circ$.

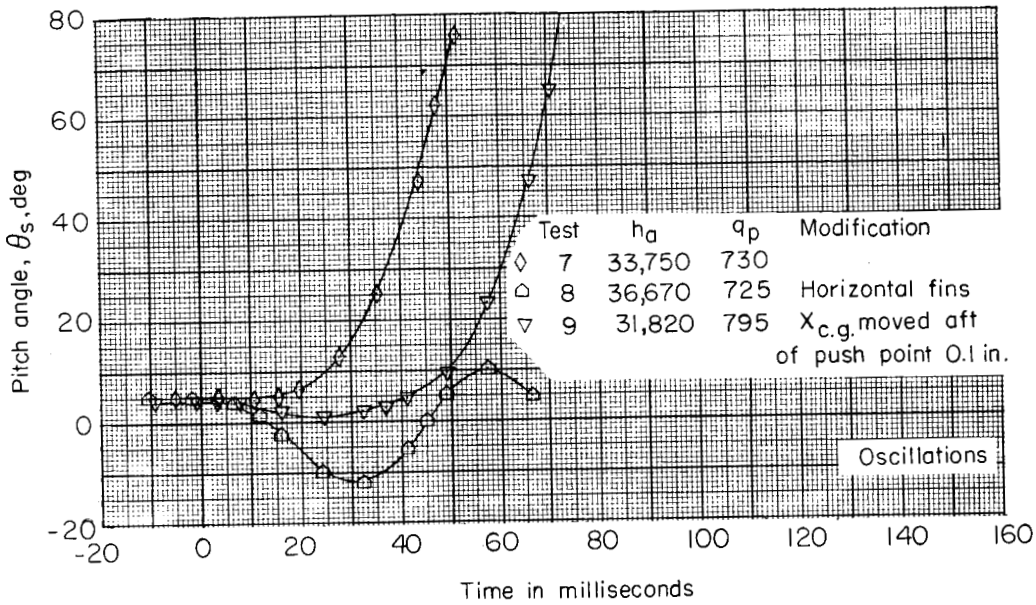

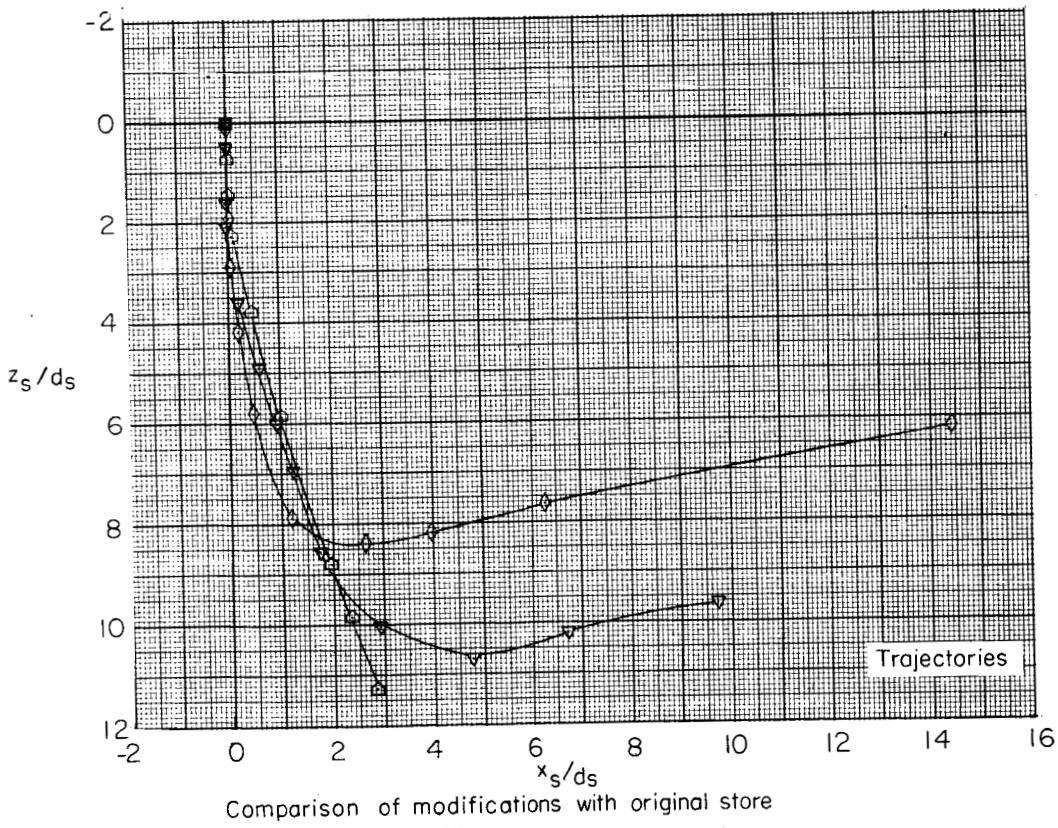

Figure 18.- Bomb 2 oscillations and trajectories. $M_\infty = 1.39$; $\alpha_w = 2^\circ$.

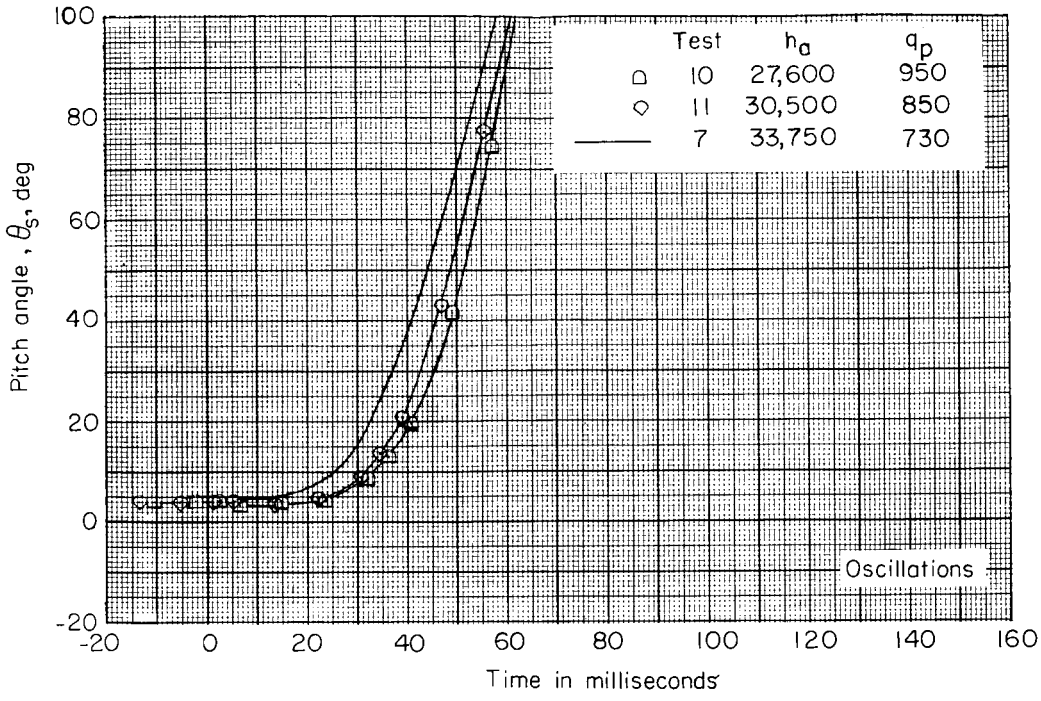

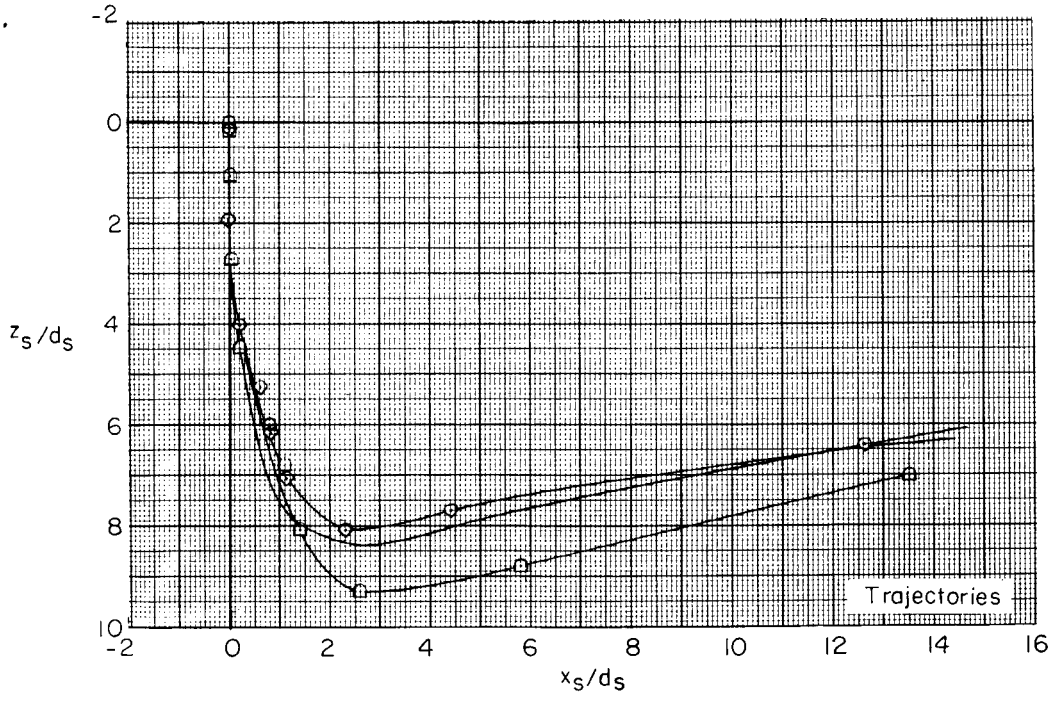

Figure 18.- Concluded.

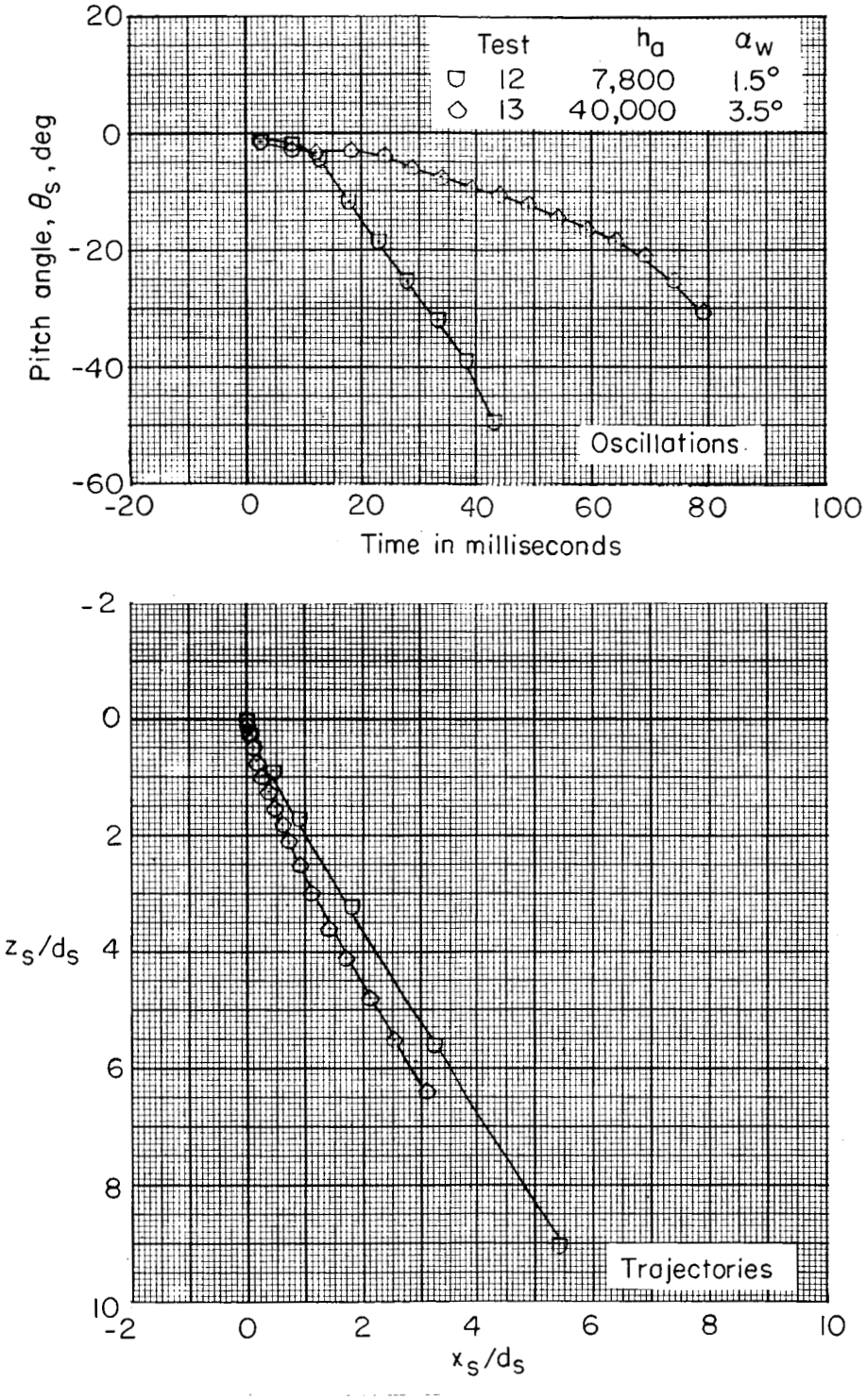

Figure 19.- Pylon tank store oscillations and trajectories. $M_\infty = 1.39$.

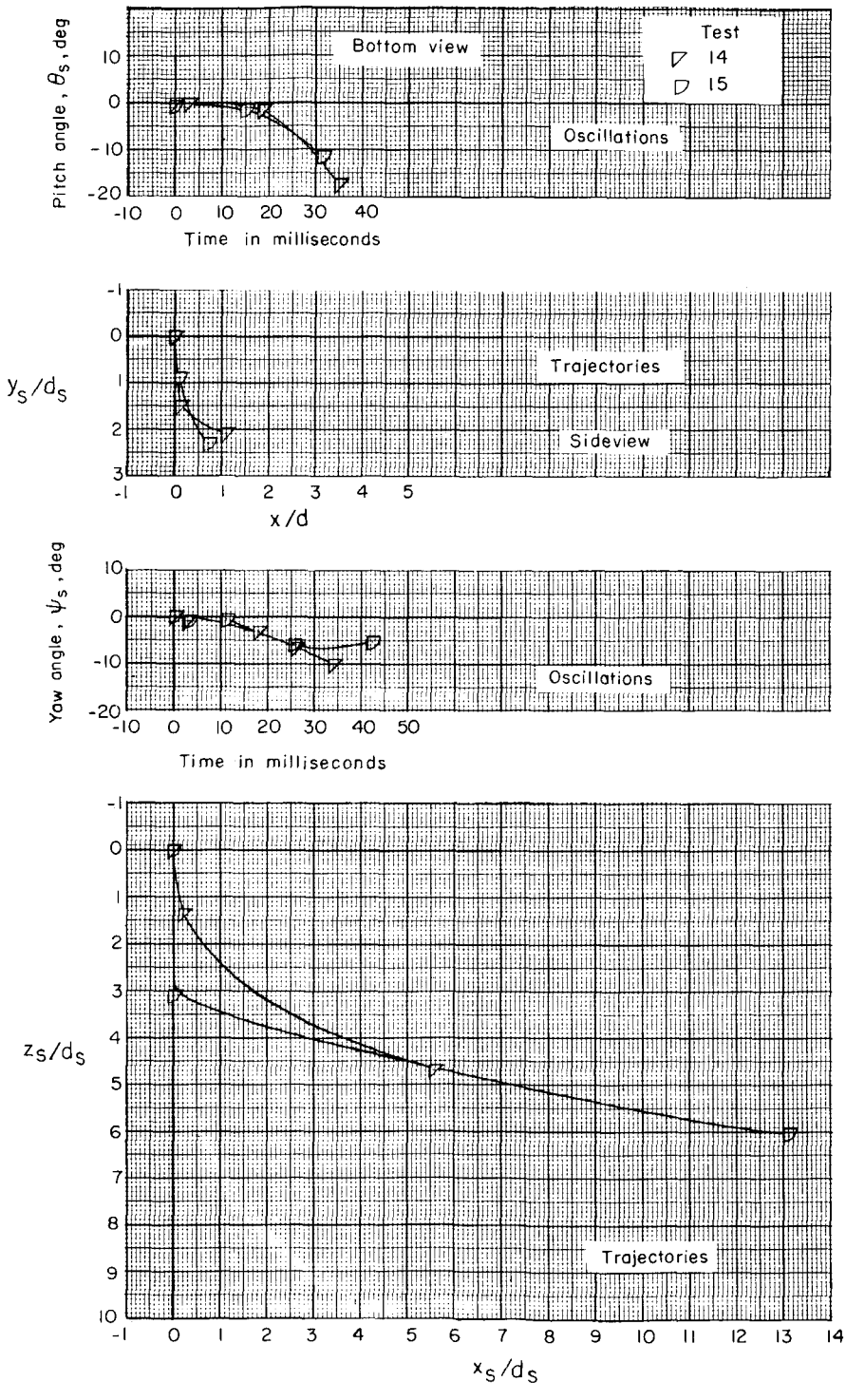

Figure 20.- Empty tip tank store oscillations and trajectories. $M_\infty = 1.39$; $h_a = 11{,}000$ feet; $\alpha_w = 1.5^\circ$.